Diversity and pathogenicity of Fusarium species associated with stalk and crown rot on maize in Northern Italy.

Martina Sanna , Ilaria Martino , Vladimiro Guarnaccia , Monica Mezzalama *

Posted Date: 9 October 2023

doi: 10.20944/preprints202310.0504.v1

Keywords: Zea mays L.; F. fujikuroi SC; F. nisikadoi SC; F. oxysporum SC; multi-locus sequence typing

Article

Diversity and Pathogenicity of *Fusarium* Species Associated with Stalk and Crown Rot on Maize in Northern Italy

Martina Sanna [1,2], Ilaria Martino [1,2], Vladimiro Guarnaccia [1,2] and Monica Mezzalama [1,2,*]

[1] Department of Agricultural, Forest and Food Sciences, University of Torino, Largo Paolo Braccini 2, 10095 Grugliasco, TO, Italy; martina.sanna@unito.it (M.S.); ilaria.martino@unito.it (I.M.); vladimiro.guarnaccia@unito.it (V.G.)

[2] AGROINNOVA—Interdepartmental Centre for the Innovation in the Agro-Environmental Sector, University of Torino, Largo Paolo Braccini 2, 10095 Grugliasco, TO, Italy; ; martina.sanna@unito.it (M.S.); ilaria.martino@unito.it (I.M.); vladimiro.guarnaccia@unito.it (V.G.)

* Correspondence: monica.mezzalama@unito.it; Tel.: +39-0116708019

Abstract: The genus *Fusarium* includes several agronomically important and toxin-producing species, that are worldwide distributed and can cause a wide range of diseases. Crown and stalk rots and grain infections are among the most severe symptoms that *Fusarium* spp. can cause on maize. The disease development usually occurs during germination, but it may also affect the later phases of plant growth. The purpose of this study was to investigate the diversity and the pathogenicity of 41 isolates recovered from symptomatic seedlings collected in Northern Italy, and from seeds with five different geographical origins during 2019 and 2020. The pathogenicity was tested and confirmed on 23 isolates causing rotting on maize seedlings. A multi-locus phylogeny analysis, based on four genomic loci (*tef1-α*, *rpb2*, *calm* and *tub2*), was performed for 23 representative isolates. Representative isolates were identified as species belonging to three species complexes (SC). *Fusarium verticillioides* and *F. annulatum* in the *F. fujikuroi* SC. *Fusarium commune* was identified in the *F. nisikadoi* SC, and three different lineages were found in the *Fusarium oxysporum* SC. This study reports *F. annulatum*, and two lineages of the *Fusarium oxysporum* SC as maize pathogens for the first time in Italy.

Keywords: *Zea mays* L.; *F. fujikuroi* SC; *F. nisikadoi* SC; *F. oxysporum* SC; multi-locus sequence typing

1. Introduction

Maize (*Zea mays* L.) is the first staple food in the world [1], and it represents the fifth most produced commodity in the European Union (EU), supplying food, feed and fuel [2]. Italy represents the tenth maize producer in EU, with 52,169,088 tons yielded in 2023 [3]. The Italian production is concentrated in the Northern regions, thus representing an economically relevant sector of agriculture for that area. Several pathogens can affect maize infecting seeds and seedlings and causing important plant diseases that lead to biosafety and phytosanitary problems and important yield and economic losses [4]. Stalk, crown and root rot are among the most severe diseases on maize [4]. Fungal species belonging to the *Fusarium* genus are one of the main causes of this disease on maize as well as on other cereals. *Fusarium* spp. are worldwide distributed and include a wide range of agronomically important and toxin-producing plant pathogens, causal agents of wilt, blight, tissues rot, and cankers of many horticultural, ornamental, and forest crops [5,6]. The infection occurs during seed germination, also affecting the plant in later growth phases, causing severe diseases, like root and stalk rot [7,8]. The disease can lead to a premature senescence and lodging of the plants, with different levels of severity depending on the pathogenic species involved, the phenological stage of the plant and the environmental conditions that occur during the cropping cycle. *Fusarium* species

 doi:10.20944/preprints202310.0504.v1

are also able to produce a wide range of mycotoxins, that accumulate in the plant tissues during the infection process, posing an important risk for human and animal health [6,8,9].

In Europe, the main species involved with maize diseases are *F. graminearum, F. culmorum*, and *F. proliferatum* [6]. Cases of root rot in maize are related to species of the *Fusarium fujikuroi* species complex (FFSC), especially to *F. verticillioides* [10]. Species belonging to the *Fusarium oxysporum* species complex (FOSC) and the *Fusarium nisikadoi* species complex (FNSC) were frequently recorded in maize seeds and seedlings [11]. *Fusarium* mycelium can survive in maize residues and seeds, and it may colonize seedlings and plants through systemic infection [12]. Previous research reported the ability of *Fusarium* species to infect seeds, transmit the pathogen through the plant and become a source of infection of the roots and stalk, up to the kernels [12–14]. The diagnosis of these diseases is often difficult due to the concurrent presence and the multiple isolation of *Fusarium* pathogens from the same symptomatic portion of the plant [15].

Currently more than 60 species belong to the FFSC, about 144 *formae specialis* are part of the FOSC, 6 species are included in FNSC, and several species are not officially assigned to a species complex [16–18]. Difficulties in *Fusarium* spp. identification lay on their morphological features, that are usually strongly influenced by environmental conditions, and on their molecular profile, because of wrong classifications of the sequences present in the public database and the nomenclature changes in the taxonomic system [19]. The molecular identification of fungi is usually obtained through sequencing of internal transcribed spacer (ITS), however, in the case of the genus *Fusarium*, ITS is exclusively able to discriminate the species complex, while the *translation elongation factor* (*tef1-α*) and the *RNA polymerase second largest subunit* (*rpb2*) genomic regions are highly informative [20,21]. Also, the *beta-tubulin* (*tub2*) and the *calmodulin* (*calm*) loci are used for *Fusarium* species identification [22]. Recently, the phylogenomic approach provided high resolution to distinguish species within the *Fusarium* genus [19]. Thus, the multi-locus phylogenetic analyses, combined with the traditional identification based on morphological methods can deepen the knowledge on this genus.

The purposes of this work, considering the economic importance of maize and the impact of *Fusarium* species on this crop, are to: (i) determine the pathogenicity of *Fusarium* spp. isolates obtained from maize seeds and seedlings, and (ii) combine phylogenetic analysis with morphological characterization of the isolates to identify and understand the diversity of the *Fusarium* species affecting maize, causing stalk and crown rot, in Northern Italy.

2. Results

2.1. Fungal isolates

The observed symptoms on maize plants consisted of browning, wilting and collapse of the seedlings, due to the decaying tissues of the stem. Disease incidence in the field was established considering the percentage of affected plants and ranged from 5 to 20%, depending on geographical location of the field. The symptoms were observed on seedlings of different maize hybrids, already at the V1 stage. Rotting kernels covered by mycelium were observed in the incubation test. The recorded percentage of seeds infected with *Fusarium* spp. in the incubation test ranged between 5 and 56%. Forty-one isolates, obtained from affected root, stem and crown tissue of the seedlings collected in the field and from the incubation test on seeds, were identified as belonging to *Fusarium* spp. (Table 1).

Table 1. *Fusarium* spp. isolates used in this study (isolate code, origin of the sample, hybrid, FAO class, symptomatic portion isolated and year of isolation).

Isolate code	Origin	Hybrid	Fao Class	Symptomatic portion	Year of isolation
DB19LUG07	San Zenone degli Ezzelini (VI)-Italy	unknown	unknown	Root	2019
DB19LUG16	San Zenone degli Ezzelini (VI)-Italy	unknown	unknown	Root	2019

Preprints (www.preprints.org) | NOT PEER-REVIEWED | Posted: 9 October 2023 doi:10.20944/preprints202310.0504.v1

DB19LUG20	San Zenone degli Ezzelini (VI)-Italy	unknown	unknown	Root	2019
DB19LUG25	San Zenone degli Ezzelini (VI)-Italy	unknown	unknown	Root	2019
2.1	Livorno Ferraris (VC)-Italy	P1547	600-130 days	Root	2019
2.2	Livorno Ferraris (VC)-Italy	P1547	600-130 days	Root	2019
8.1	Cigliano (VC)-Italy	-	-	Root	2019
8.2	Cigliano (VC)-Italy	-	-	Root	2019
9	USA	PR32B10	600-132 days	Seed	2019
10.1	France	P0423	400-116 days	Seed	2019
10.2	France	P0423	400-116 days	Seed	2019
11	Italy	unknown	unknown	Seed	2019
12	Italy	SY ANTEX	600-130 days	Seed	2019
18	Turkey	DKC6752	600-128 days	Seed	2019
19	Romania	DKC5830	500-x days	Seed	2019
21	Crescentino (VC)-Italy	P1547	600-130 days	Stem	2019
23	Crescentino (VC)-Italy	P1547	600-130 days	Root	2019
24	Crescentino (VC)-Italy	P1916	600-130 days	Root	2019
26	Crescentino (VC)-Italy	P1916	600-130 days	Stem	2019
28	Crescentino (VC)-Italy	P1916	600-130 days	Root	2019
29	Cigliano (VC)-Italy	P1517W	600-128 days	Root	2019
30	Cigliano (VC)-Italy	P1517W	600-128 days	Root	2019
31	Cigliano (VC)-Italy	P1517W	600-128 days	Stem	2019
32	Cigliano (VC)-Italy	P1517W	600-128 days	Stem	2019
35.1.4	Cigliano (VC)-Italy	P1517W	600-128 days	Root	2019
36	Cigliano (VC)-Italy	P1517W	600-128 days	Stem	2019
40	Cigliano (VC)-Italy	P1517W	600-128 days	Root	2019
41	Cigliano (VC)-Italy	P1547	600-130 days	Root	2019
44	Cigliano (VC)-Italy	P1547	600-130 days	Root	2019
50	Cigliano (VC)-Italy	P1547	600-130 days	Root	2019
51	Cigliano (VC)-Italy	unknown	unknown	Stem	2019
55.2.1	Cigliano (VC)-Italy	unknown	unknown	Crown	2019
56.1.2	Cigliano (VC)-Italy	unknown	unknown	Root	2019
56.2.2	Cigliano (VC)-Italy	unknown	unknown	Root	2019
56.2.3	Cigliano (VC)-Italy	unknown	unknown	Root	2019
56.2.4	Cigliano (VC)-Italy	unknown	unknown	Root	2019
56.2.5	Cigliano (VC)-Italy	unknown	unknown	Root	2019
57.2.1	Cigliano (VC)-Italy	unknown	unknown	Root	2019
1.RI (Pta 1.1)	San Zenone degli Ezzelini (VI)-Italy	unknown	unknown	Crown	2020
1.RI (Pta 1.2)	San Zenone degli Ezzelini (VI)-Italy	unknown	unknown	Crown	2020
1.RII (Pta 3.2)	San Zenone degli Ezzelini (VI)-Italy	unknown	unknown	Crown	2020

2.2. Pathogenicity test

A total of 36 out of 41 isolates tested caused root and crown rot like those observed in the field during spring 2019 and 2020 (Figure 1).

Preprints (www.preprints.org) | NOT PEER-REVIEWED | Posted: 9 October 2023 doi:10.20944/preprints202310.0504.v1

Figure 1. Symptoms caused by *Fusarium* spp. (**A**, **B**) observed in the field and (**C**, **D**) after pathogenicity trials on leaves, roots and crowns maize seedlings.

Different severity indexes, depending on the isolate tested, were observed. A total of 19 isolates showed disease indexes ranging from 13.3% to 46.7%, and only 17 of them showed a disease index higher than 50% (Table 2).

Table 2. Results of pathogenicity test performed on the 41 *Fusarium* isolates isolated, at 14 days. Number of plants recorded for each index and disease index (0–100) of each isolate (ANOVA and Duncan $p < 0.05\%$).

ID Sample	Severity index of root and crown rot (number of plant)					Disease index	
	1	2	3	4	5	(DI) 0-100	
DB19LUG07	0	3	3	0	0	50.0	abcde
DB19LUG16	0	6	0	0	0	40.0	cdefg
DB19LUG20	4	2	0	0	0	13.3	gh
DB19LUG25	3	3	0	0	0	20.0	gh

Preprints (www.preprints.org) | NOT PEER-REVIEWED | Posted: 9 October 2023 doi:10.20944/preprints202310.0504.v1

2.1	0	0	0	4	2	86.7	a
2.2	0	0	0	3	3	90.0	a
8.1	6	0	0	0	0	0.0	h
8.2	3	3	0	0	0	20.0	fgh
9	0	0	0	6	0	80.0	ab
10.1	0	0	2	0	4	86.7	a
10.2	0	0	1	2	3	86.7	a
11	3	3	0	0	0	20.0	efgh
12	0	3	0	0	3	70.0	abc
18	2	3	0	0	1	36.7	efgh
19	6	0	0	0	0	0.0	h
21	2	4	0	0	0	26.7	efgh
23	2	4	0	0	0	26.7	efgh
24	0	3	0	0	3	70.0	abc
26	0	4	2	0	0	46.7	bcdef
28	3	3	0	0	0	20.0	efgh
29	0	6	0	0	0	40.0	cdefg
30	3	3	0	0	0	20.0	efgh
31	2	4	0	0	0	26.7	efgh
32	4	2	0	0	0	13.3	gh
35.1.4	0	1	1	2	2	76.7	abc
36	3	3	0	0	0	20.0	efgh
40	0	4	2	0	0	46.7	bcdef
41	6	0	0	0	0	0.0	h
44	6	0	0	0	0	0.0	h
50	6	0	0	0	0	0.0	h
51	2	2	2	0	0	33.3	defgh
55.2.1	0	1	1	2	2	76.7	abc
56.1.2	0	0	0	4	2	86.7	a
56.2.2	0	0	2	2	2	80.0	ab
56.2.3	0	0	0	3	3	90.0	a
56.2.4	0	0	2	2	2	80.0	ab
56.2.5	0	0	2	4	0	73.3	abc
57.2.1	0	0	0	4	2	86.7	a
1.RI (Pta 1.1)	2	2	0	0	2	46.7	cdefg
1.RI (Pta 1.2)	0	2	2	0	2	66.7	abcd
1.RII (Pta 3.2)	3	3	0	0	0	20.0	efgh
Healthy control	6	0	0	0	0	0.0	h

The identity of the re-isolated fungi was proved by sequencing the *tef-1α* locus, confirming the Koch's postulates. No symptoms were observed on healthy control plants. A total of 23 out of 36 pathogenic isolates were selected as representative isolates, based on their cultural features, to proceed with molecular analyses and their characterization.

2.3. Phylogenetic analyses

The preliminary analysis conducted on the obtained sequences showed that the 23 selected isolates belong to three *Fusarium* species complexes, *Fusarium fujikuroi* SC, *Fusarium nisikadoi* SC and *Fusarium oxysporum* SC. The combined phylogeny analyses of *tef-1α*, *rpb2*, *calm* and *tub2* performed for FFSC isolates consisted of 101 sequences, including the outgroup sequence of *Fusarium foetens* (CBS 120665). A total of 2210 characters (*tef-1α*: 1-621, *rpb2*: 628-1185, *calm*: 1192-1726, *tub2*: 1733-2210) were included in the analysis: 563 characters resulted as parsimony-informative, 604 as variable and parsimony uninformative, and 1025 were constant. A maximum number of 1000 equally most

Preprints (www.preprints.org) | NOT PEER-REVIEWED | Posted: 9 October 2023 doi:10.20944/preprints202310.0504.v1

parsimonious trees were saved (Tree length = 2973, CI = 0.602, RI = 0.812 and RC = 0.488). Bootstrap support values obtained with the parsimony analysis are showed on the Bayesian phylogenies in Figure 2. Bayesian analyses, the dirichlet state frequency distributions were suggested by MrModeltest for analysing all the partitions. The following models, recommended by MrModeltest, were used: GTR+G for *tef-1α*, SYM+I+G for *rpb2*, SYM+G for *calm*, and HKY+G for *tub2*. In the Bayesian analysis, the *tef1-α* partition had 370 unique site patterns, the *rpb2* partition had 191 unique site patterns, the *calm* partition had 233 unique site patterns, the *tub2* partition had 269 unique site patterns and the analysis ran for 405000 generations, resulting in 812 trees of which 305 trees were used to calculate the posterior probabilities. In the combined analyses eight isolates clustered with seven reference isolates of *F. verticillioides*, while six isolates were grouped with 3 isolates known as reference of *F. annulatum* [19].

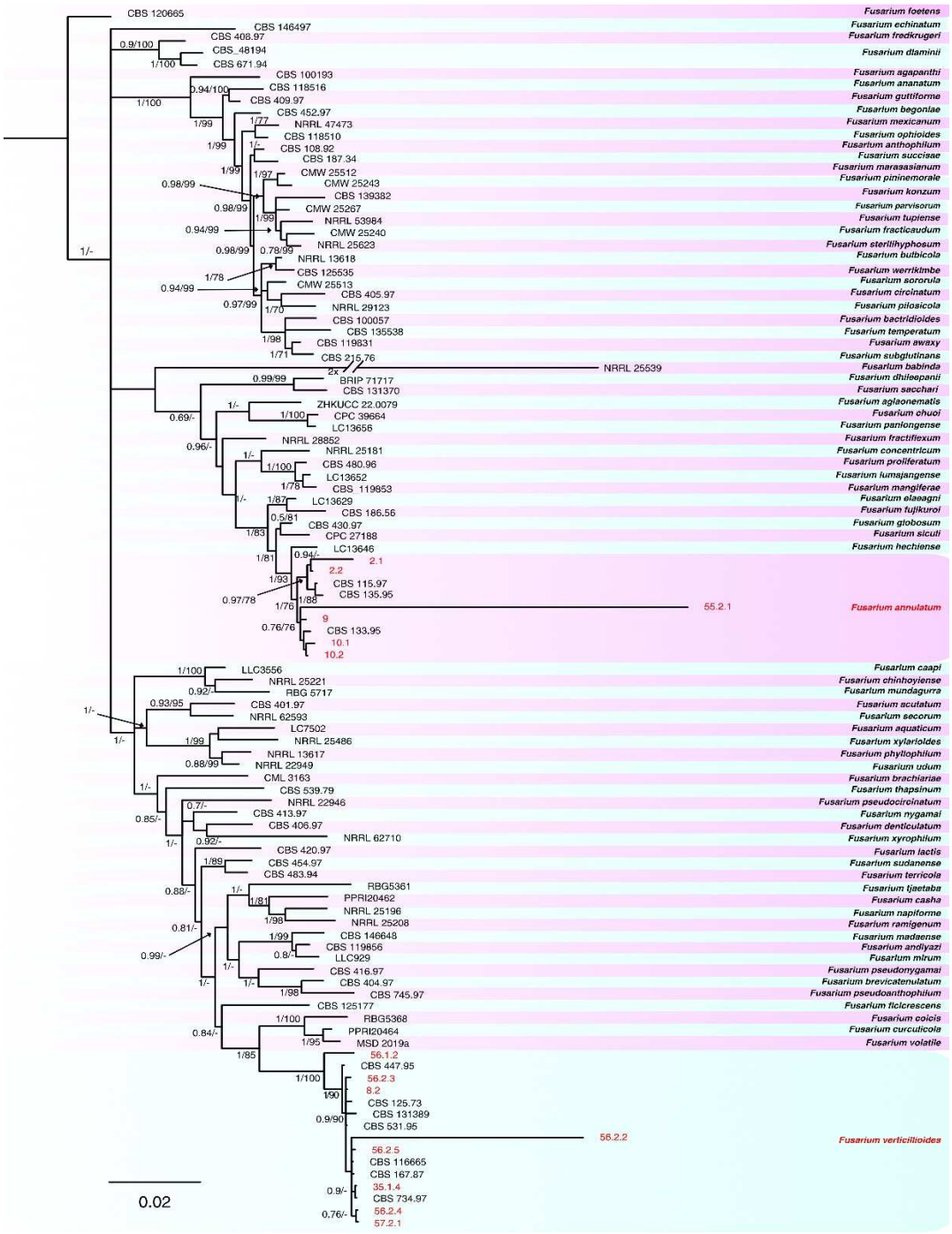

Figure 2. Consensus phylogram of 305 trees resulting from a Bayesian analysis of the combined *tef1-α*, *rpb2*, *calm* and *tub2* sequences of *Fusarium* spp. belonging to FFSC. Bayesian posterior probability

Preprints (www.preprints.org) | NOT PEER-REVIEWED | Posted: 9 October 2023 doi:10.20944/preprints202310.0504.v1

values and Bootstrap support values are indicated at the nodes. The isolates collected and species found in this study are in red. The tree was rooted to *Fusarium foetens* (CBS 120665).

The combined phylogeny analysis of the three loci (*tef-1α*, *rpb2* and *calm*) performed for FOSC isolates consisted of 47 sequences, including the outgroup sequence of *Fusarium udum* (NRRL22949). A total of 1762 characters (*tef-1α*: 1-589, *rpb2*: 596-1231, *calm*: 1238-1762) were included in the analysis: 77 characters resulted as parsimony-informative, 171 as variable and parsimony uninformative, and 1502 were constant. A maximum number of 1000 equally most parsimonious trees were saved (Tree length = 297, CI = 0.882, RI = 0.892 and RC = 0.787). Bootstrap support values obtained with the parsimony analysis are showed on the Bayesian phylogenies in Figure 3. For the Bayesian analyses, the dirichlet state frequency distributions were suggested by MrModeltest for analysing all the partitions. The following models, recommended by MrModeltest, were used: HKY for *tef-1α*, K80 for *rpb2*, and *calm*. In the Bayesian analysis, the *tef1-α* partition had 109 unique site patterns, the *rpb2* partition had 71 unique site patterns, the *calm* partition had 57 unique site patterns and the analysis ran for 300000 generations, resulting in 602 trees of which 226 trees were used to calculate the posterior probabilities. In the combined analyses one isolate clustered with four reference isolates and the ex-type of *F. nirenbergiae*, one isolate was identified as *F. cugenangense*, while five isolates were identified as *F. oxysporum sensu lato*, cause they not cluster with anyone of reference sequences, according with the recent taxoxonomy revision of this SC reported by Lombard et al. [17].

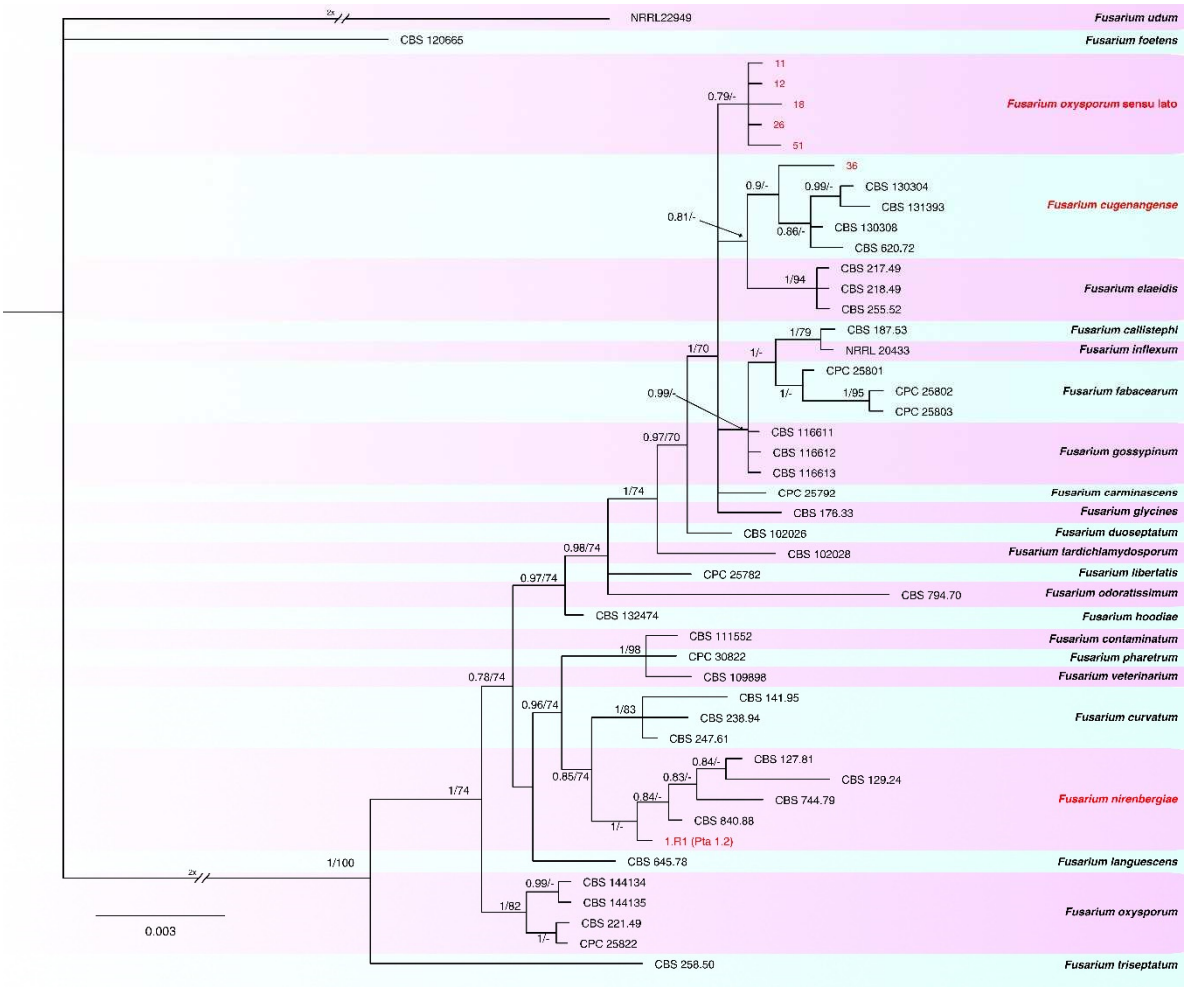

Figure 3. Consensus phylogram of 226 trees resulting from a Bayesian analysis of the combined *tef1-α*, *rpb2* and *calm* sequences of *Fusarium* spp. belonging to FOSC. Bayesian posterior probability values and Bootstrap support values are indicated at the nodes. The isolates collected and species found in this study are in red. The tree was rooted to *Fusarium udum* (NRRL22949).

Preprints (www.preprints.org) | NOT PEER-REVIEWED | Posted: 9 October 2023 doi:10.20944/preprints202310.0504.v1

The combined phylogeny analysis of the four loci (*tef-1α*, *rpb2*, *calm* and *tub2*) performed for FNSC isolates consisted of 15 sequences, including the outgroup sequence of *Fusarium udum* (NRRL22949). A total of 2024 characters (*tef-1α*: 1-585, *rpb2*: 592-1362, *calm*: 1369-1594, *tub2*: 1601-2024) were included in the analysis, 186 characters resulted as parsimony-informative, 333 as variable and parsimony uninformative, and 1487 were constant. A maximum number of 1000 equally most parsimonious trees were saved (Tree length = 616, CI = 0.959, RI = 0.922 and RC = 0.884). Bootstrap support values obtained with the parsimony analysis are showed on the Bayesian phylogenies in Figure 4. For the Bayesian analyses, the dirichlet state frequency distributions were suggested by MrModeltest for analysing all the partitions. The following models, recommended by MrModeltest, were used: HKY for *tef-1α*, HKY+G for *rpb2*, JC for *calm*, and SYM+G for *tub2*. In the Bayesian analysis, the *tef1-α* partition had 106 unique site patterns, the *rpb2* partition had 47 unique site patterns, the *calm* partition had 19 unique site patterns, the *tub2* partition had 57 unique site patterns and the analysis ran for 400000 generations, resulting in 802 trees of which 301 trees were used to calculate the posterior probabilities. In the combined analyses two isolates clustered with seven reference isolates of *F. commune*.

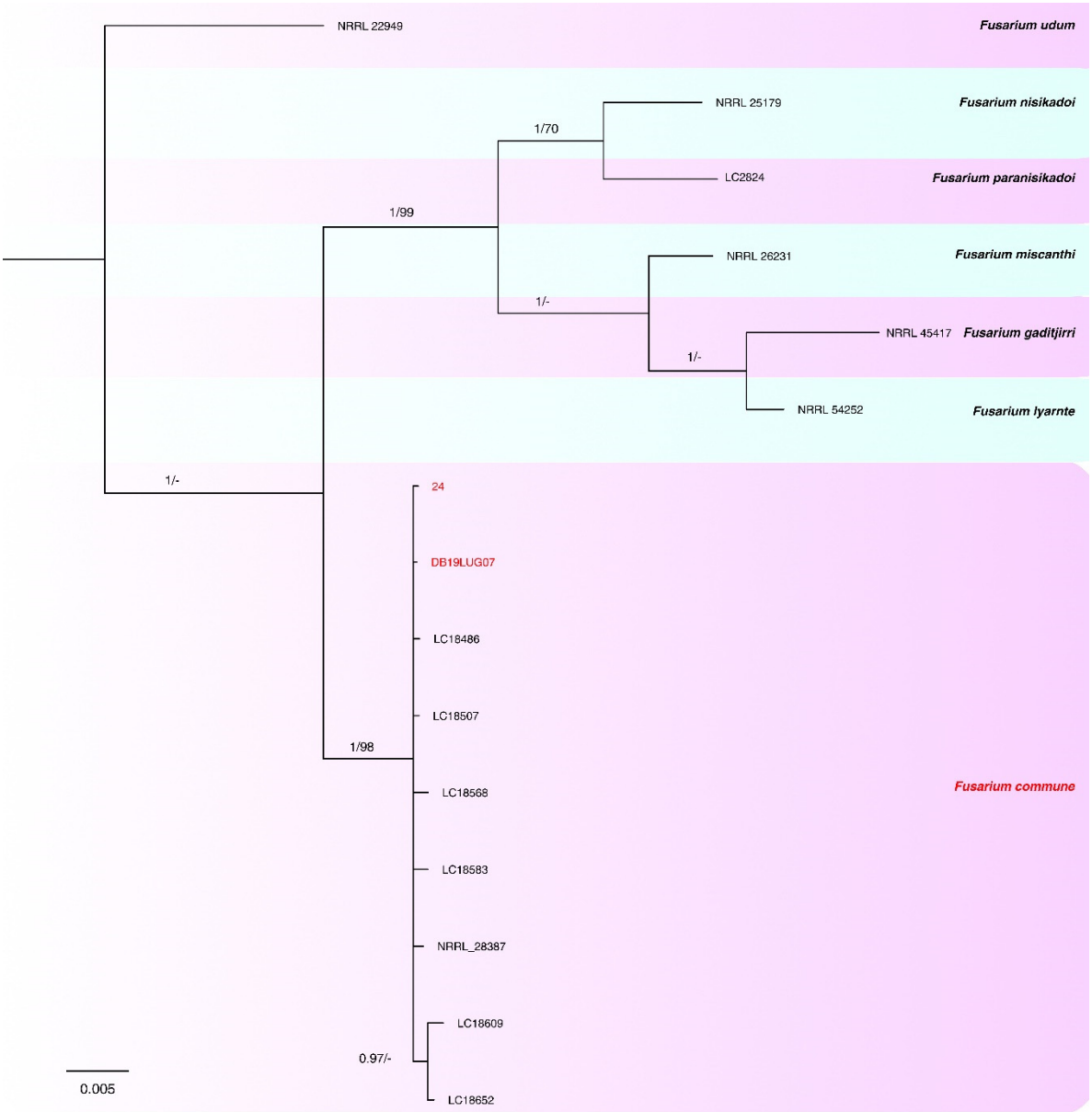

Figure 4. Consensus phylogram of 301 trees resulting from a Bayesian analysis of the combined *tef1-α*, *rpb2*, *calm* and *tub2* sequences of *Fusarium* spp. belonging to FNSC. Bayesian posterior probability

Preprints (www.preprints.org) | NOT PEER-REVIEWED | Posted: 9 October 2023 doi:10.20944/preprints202310.0504.v1

values and Bootstrap support values are indicated at the nodes. The isolates collected and species found in this study are in red. The tree was rooted to *Fusarium udum* (NRRL22949).

2.4. Morphology

Morphological features, supported by phylogenetic analysis, were assessed, and used to characterize 6 species, belonging to three species complexes, found in this study. (Figures 5-7).

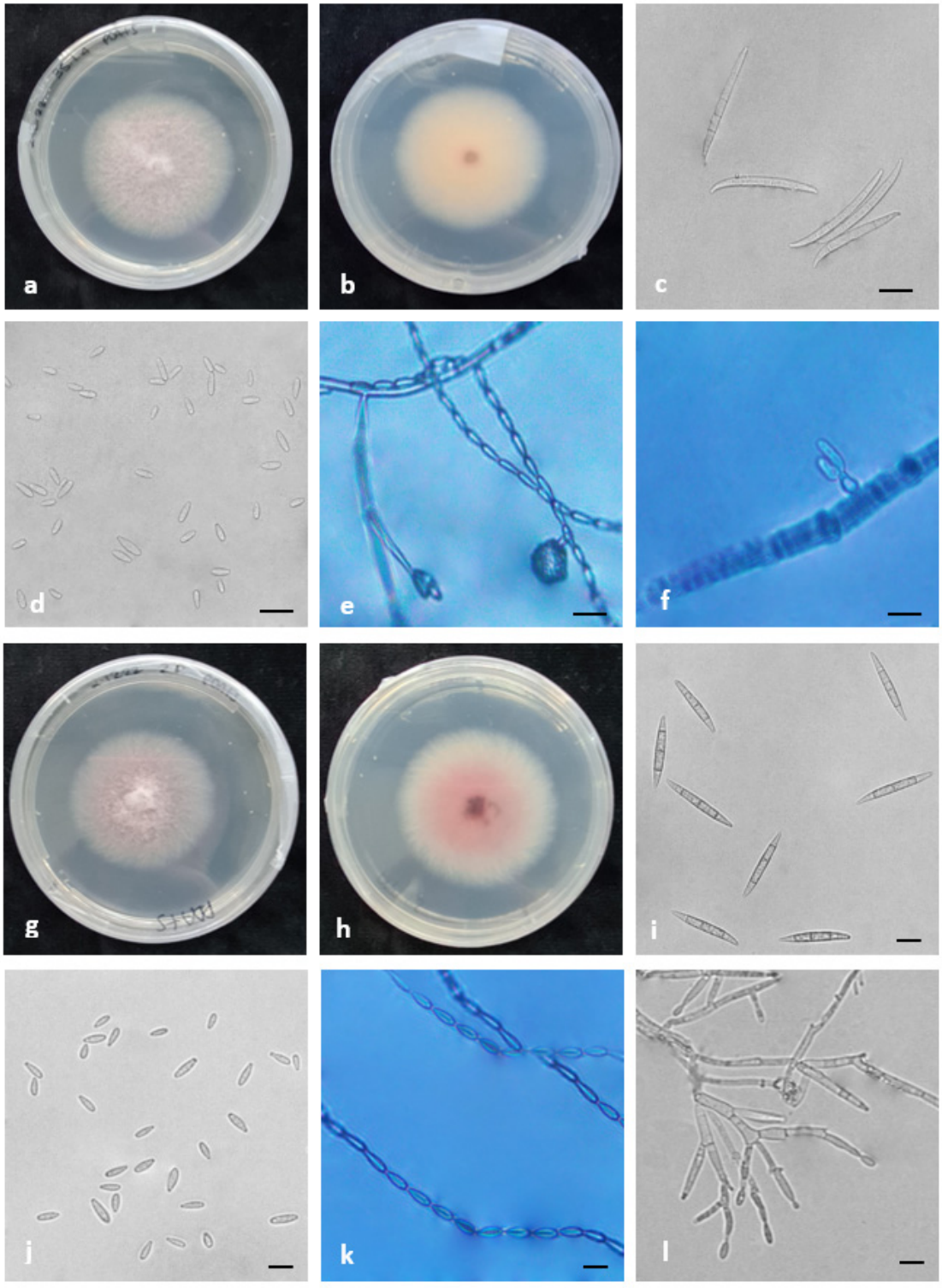

Figure 5. Morphological features of the species belonging to FFSC identified in this study. (**A**, **B**, **C**, **D**, **E**, **F**) *F. verticillioides* and (**G**, **H**, **I**, **J**, **K**, **L**) *F. annulatum*. a-b-g-h. Colonies on PDA above and below; c–d-e-i-j-k. conidia; f-l. conidiogenous cells.— Scale bars = 10 μm.

Preprints (www.preprints.org) | NOT PEER-REVIEWED | Posted: 9 October 2023 doi:10.20944/preprints202310.0504.v1

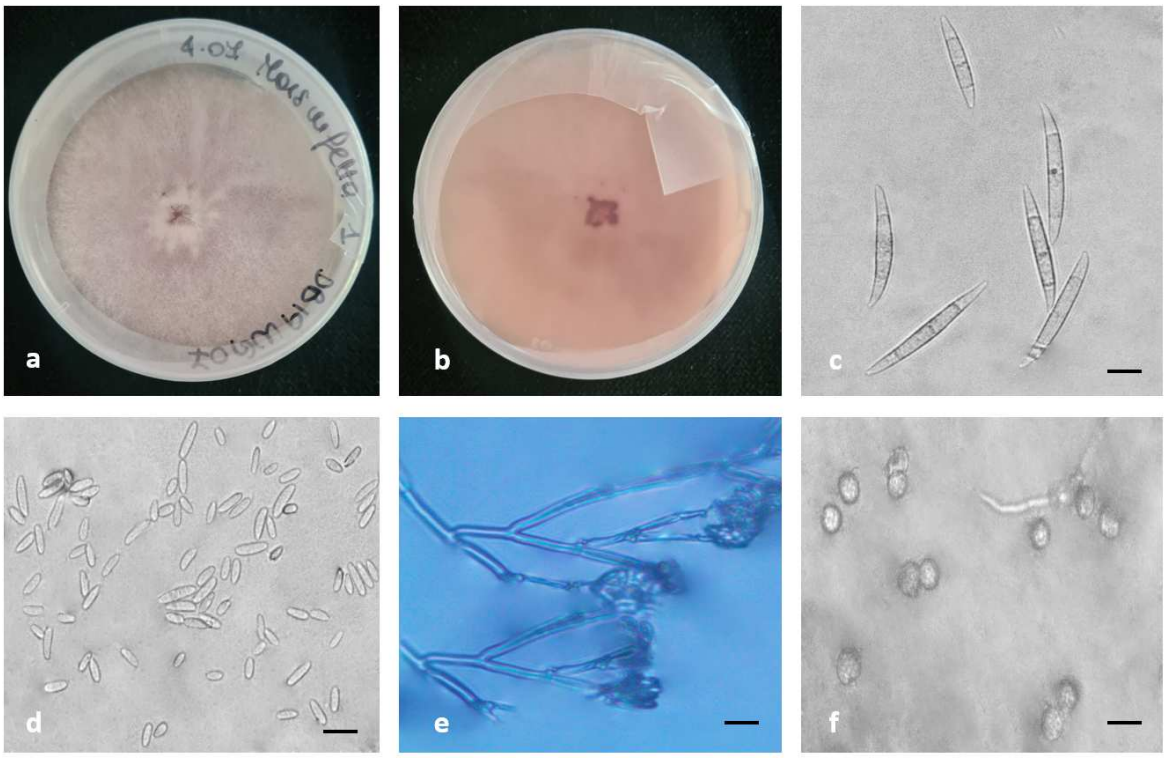

Figure 6. Morphological features of *F. commune*, the species belonging to FNSC identified in this study. a-b. Colonies on PDA above and below; c–d. conidia; e. conidiogenous cells; f. chlamydospores.— Scale bars = 10 µm.

Seven-day-old colonies of *F. verticillioides* showed white abundant aerial mycelium that developed violet pigments with age. Colony radius was 55–70 mm. Monophialides were produced and appeared in V-shaped pairs, similar to "rabbit ears". Microconidia were hyaline, oval to club shaped, aseptate, (6-)7-12(-13) x 2.5-3.5 µm (mean 7 x 3.0 µm), abundant in aerial mycelium and disposed in long chains. Macroconidia were straight and slender, with the apical cell foot-shaped, 4-6 septate, hyaline, (28-)32-49(-52) x 2.5-3 µm (mean 38.5 x 3.0 µm). Chlamydospores were absent.

F. annulatum colonies, after 7 days at 25°C on PDA reached 50-60 mm diameter. The surface was characterized by white aerial mycelium that became darker with age, while the reverse showed intense pink to purple pigments at the center of the colony. Conidiophores produce mono and polyphialides, which generates a large number of microconidia that could be grouped in long chains, on CLA. Microconidia are formed on aerial conidiophores, hyaline, oval to elliptical, aseptate, (2-)5-12(-15) x 1.5-3.5 µm (mean 8.8 x 2 µm). Macroconidia are hyaline, slender, straight to curve, with foot-shaped apical cell, 4-5 septate, (30-)35-42(-54) x 2-4 µm (mean 37 x 3 µm). Chlamydospores are absent.

F. commune colonies morphology was characterized by white to pink, abundant, floccose to fluffy mycelium on the surface and by violet pigmentation on the reverse colony. After 7 days of incubation at 25°C colony radial growth reach 45-50 mm, on PDA. *F. commune* produced both, mono and polyphialides. On CLA the isolates produced slightly curved 3-4 septate macroconidia (23-)28-56(-66) x 2.5-6 µm (mean 38.5 x 4 µm) and aseptate, cylindrical, and straight microconidia (3.5-)5-7(8.2) x 2-3 µm (mean 6 x 2.5 µm). Chlamydospores were produced, single or in pairs.

F. nirenbergiae colony radial growth measure 55-60 mm, after 7 days on PDA. The colony surface was characterized by an abundant pink and floccose mycelium, and by greyish pink pigments on the reverse. Conidiophores carried on the aerial mycelium produced monophialides that bears oval, aseptate microconidia (8-)9-15(-16.2) x 2-3.5 µm (mean 11.2 x 3.2 µm), and 3-4 septate, slender, straight, with a papillate apical cell and a foot shaped basal cell (26.5-)28-30(-32.2) x 2.5-4.8 µm (mean 28.5 x 3.4 µm) macroconidia. Globose chlamydospores were produced.

Preprints (www.preprints.org) | NOT PEER-REVIEWED | Posted: 9 October 2023 doi:10.20944/preprints202310.0504.v1

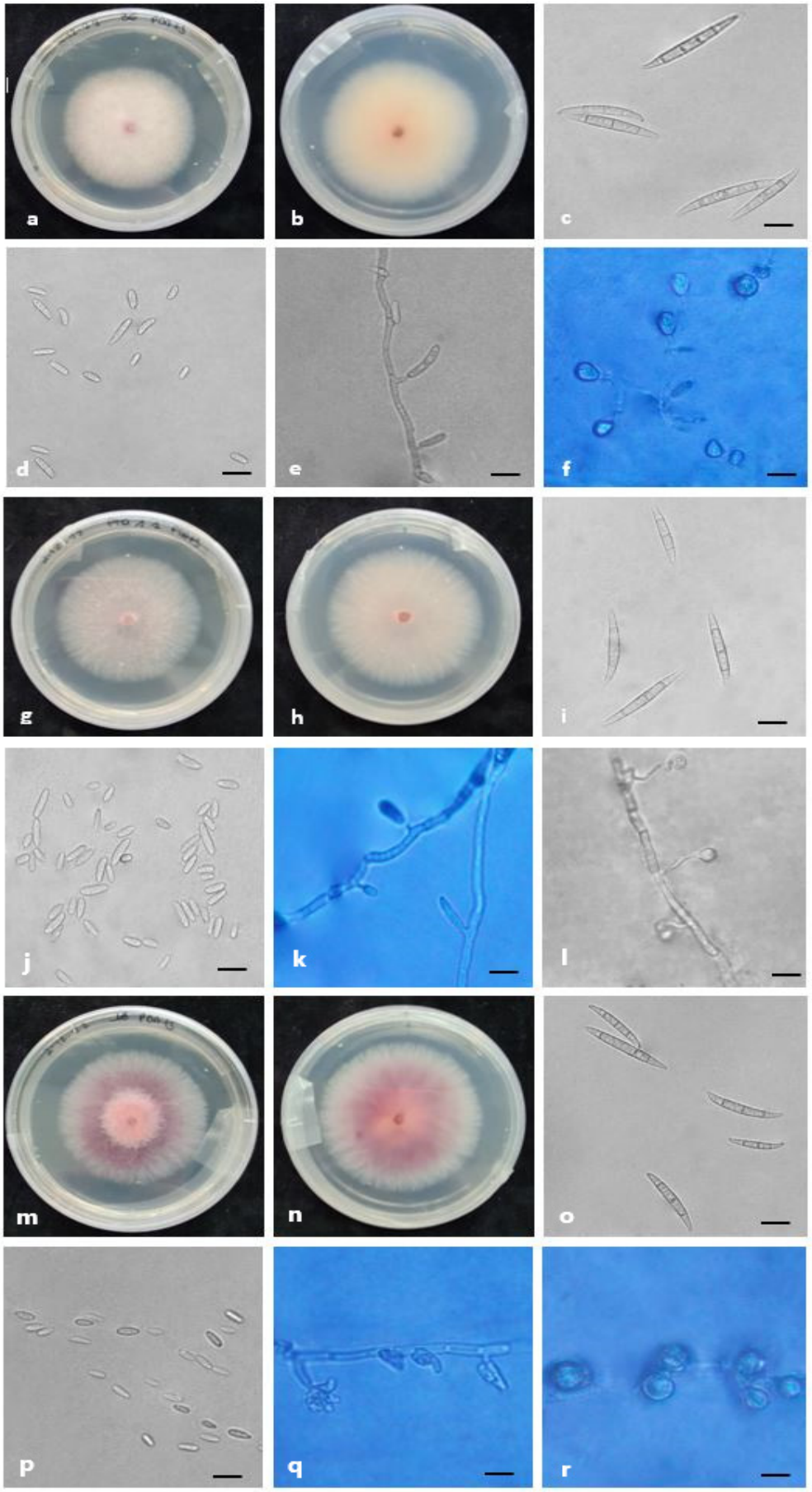

Figure 7. Morphological features of the species belonging to FOSC identified in this study, (**A, B, C, D, E, F**) *F. cugenangense,* (**G, H, I, J, K, L**) *F. nirenbergiae,* and (**M, N, O, P, Q, R**) *F. oxysporum sensu lato.*

 doi:10.20944/preprints202310.0504.v1

a-b-g-h-m-n. Colonies on PDA above and below; c–d-i-j-o-p. conidia; e-k-q. conidiogenous cells; f-l-r. chlamydospores.— Scale bars = 10 μm.

One isolate was identified as *F. cugenangense*, which colony morphology on PDA was characterized by white to pink, abundant, and cottony mycelium on the surface and pink at center to pale grey on colony reverse. Colony radius, after 7 days at 25°C under 12-h photoperiod on PDA, was 40–56 mm. It was characterized by monophialidic conidiogenous cells that produced 3-6 septate macroconidia (42.5-)46-55(-56.2) x 5.5-6.5 μm (mean 50.2 x 6 μm), with papillate apical cells and foot-shaped basal cells. Microconidia were abundant, oval to elliptical, 0-3 septate (7-)8.3-10.5(-13) x 4-7.5 μm (mean 9 x 5.6 μm). Chlamydospores are globose and formed single or in pairs.

The isolates classified as *F. oxysporum sensu lato* were characterized by an abundant pink to purple and floccose mycelium, and by purple to red pigments on the reverse. Colony radius was 50–60 mm after 7 days at 25°C under 12-h photoperiod on PDA. The isolates were characterized by conidiophores that produced monophialides, that bears slender, straight, 3-5 septate, with foot shaped basal cells and papillate apical cells macroconidia (29-)30-37(-44) x 3-4.5 μm (mean 35 x 3.8 μm). Microconidia were abundant, oval, aseptate (5.5-)6-11(-15) x 2-3 μm (mean 9.2 x 2.5 μm). Single chlamydospores were formed.

3. Discussion

Several species of *Fusarium* represent a severe problem for cereals cultivation and production worldwide causing relevant yield and economic losses and posing a serious threat to human and animal health due to their ability to produce mycotoxins [4].

In the present study, *Fusarium* spp. were isolated from maize seedlings with symptoms of root and crown rot in Northern Italy, and from rotted kernels collected in 5 different countries with the aim to investigate their diversity and pathogenicity. Isolates from seed were included, due to the ability of *Fusarium* species to be seed borne and seed transmitted [12,23], causing stalk, crown and root rot that can be observed in the field under favorable soil moisture and temperature conditions. A polyphasic approach was used to study the fungal isolates obtained from the affected plants including the analysis of multiple characters, since the morphological features alone, which represent the traditional identification method used for *Fusarium* spp. identification, are not enough to discriminate among species [16]. The combination of multi-locus sequence analysis, pathogenicity data and morphological characteristics, represent the best way to characterize fungi at species level. According to O'Donnell et al. [24], ITS region is not able to distinguish *Fusarium* species boundaries and for this reason was not considered in this study. The *tef1-α*, *rpb2*, *tub2* and *calm* loci were used for *Fusarium* spp. identification, according to the previous phylogenetic analysis of the genus reported in literature [16,17,19]. Six different species were identified in association with infection of crown, root and seeds of maize: *F. verticillioides* and *F. annulatum* belonging to the FFSC, *F. commune* belonging to the FNSC, and three different lineages in the FOSC. The FFSC contains 84 described species, including a large number of cryptic species identifiable only based on phylogenetic inference [16,18,19]. The complex includes important plant pathogens and toxin-producers [16], and species belonging to FFSC can be discriminated from other complexes due to the production of macroconidia, a large amount of microconidia and sporadically of chlamydospore [19]. The results obtained in this study allowed the classification of 14 isolates in this complex, identified as *F. verticillioides* and *F. annulatum*.

Fusarium verticillioides is one of the most important species that affects maize, it is worldwide distributed and it can cause important yield and grain quality losses [25]. It is primarily reported as the causal agent of the ear rot on maize, however studies also reported the pathogen as responsible of symptoms of seedlings decay, and stalk, crown, and root rot on maize [19,26,27]. *F. annulatum*, firstly described by Bugnicourt et al. [28], is a species associated with symptoms of rot on different crops, such as cantaloupe melons in Spain or saffron in China [29,30]. The name *F. annulatum* is often confused with *F. proliferatum*, a well-known maize pathogen, associated with crown and root rot [15,31]. A phylogenetic analysis based on LSU, SSU, and *tub2* genomic loci showed that the reference

sequence of *F. annulatum* (CBS 258.54) introduced by Bagnicourt [28], clustered with representative strains of *F. proliferatum* (CBS 217.76, NRRL 25089) [32]. These results led to the wide report of *F. proliferatum*, instead of *F. annulatum*, as maize pathogen. However, a recent multi-locus phylogenetic analyses based on *calm*, *rpb1*, *rpb2*, and *tef1-α* loci, including the epitype of *F. proliferatum* (CBS 480.96), established that this species clustered distant from *F. annulatum* [19]. The same study demonstrated that several cereals pathogenic isolates, identified as *F. proliferatum* in previous researches [15,31,33], should be identified as *F. annulatum*. The present research, based on the taxonomic characterization of Yilmaz et al. [16], demonstrated the characterization of the pathogenic isolates as the species *F. verticillioides* and *F. annulatum,* which belong to the same species complex and represent the highest proportion of the pathogenic isolates infecting maize samples considered in this study. To our knowledge this is the first report of *F. annulatum* as causal agent of stalk, crown and root rot on maize, in Italy. *Fusarium commune* belongs to FNSC and it is principally known as a pathogen of rice and maize [34]. Its behavior as pathogen is similar to those of some species belonging to FOSC, causing rot and wilt of the plants [19]. Recent studies reported *F. commune* as causal agent of stalk, crown and root rot on maize in Italy [35], and in Liaoning province in China [36]. The phylogenetic analysis conducted by Skovgaard et al. [37] identified the species as a sister group to FOSC, a result supported by the high morphological similarity between these taxa. Species of FNSC could be distinguished from those of FOSC only because of the presence of long and thin monophialides and the occasional production of polyphialides [34,37]. To discriminate and identify the species the *tef1-α* genomic region was used, due to its high phylogenetic signal [34]. *Fusarium oxysporum* is an economically important soilborne and ubiquitous plant pathogen, that covers the fifth place in the top ten rank of the most important phytopathogens [38], and it is mainly known as causal agent of plant wilts. The challenge in identification of the species belonging to this complex is due to the inability to discriminate them on the basis of morphological features, the affected wide host range and their geographical distribution [39,40]. The *tef1-α* and *rpb2* genomic loci provided the best resolution in distinguishing the species, as seen by Lombard et al. [17]. The *calmodulin* provided a little support, while the *β-tubulin* was excluded. Considering the current literature [17,19], the multi-locus phylogenetic analysis performed in this study allowed to identify seven isolates within three lineages of FOSC. The first lineage includes one isolate which formed a well-supported clade with the reference isolate and the ex-type of *F. nirenbergiae*. The second lineage includes one isolate which clustered with reference of *F. cugenangense*. Whilst the third lineage includes five isolates that did not cluster with any of the reference species used for the phylogenetic analyses and that were defined as *F. oxysporum sensu lato*. *Fusarium nirenbergiae* belongs to FOSC and it is reported as pathogen on saffron in China [30], and on passion fruit in Italy [41]. It was recently described as pathogen on maize in China [19], and our study represents the first finding of this species as maize pathogen in Italy. It is closely related to *F. curvatum*, and it can be morphologically distinguished from this species by the production of monophialidic conidiogenous cells and the production of chlamydospores, that are absent in *F. curvatum* [17]. For the species identification, morphological features must be supported by phylogenetic inference. The *tef-1α* and the *rpb2* gene regions provided the best resolution to distinguish the species [17]. *Fusarium cugenangense* was previously included in the species *F. oxysporum* f. sp. *cubense*, the causal agent of banana wilt, however phylogenetic analyses distinguished this lineage as a new independent species [42]. This pathogen has a wide host range, such as *Acer palmatum*, *Crocus* sp., *Gossypium barbadense*, *Hordeum vulgare*, *Solanum tuberosum*, *Smilax* sp., *Tulipa gesneriana*, *Musa nana*, *Musa* sp., *Vicia faba* and *Zea mays* [18,19,42]. To our knowledge, this is the first report of *F. cugenangense* as pathogen of *Zea mays* in Italy. This species is closely related to *F. callisthephi, F. elaeidis*, and to other *formae speciales*, however it can be discriminated from the other species under the morphological point of view, due the septation of the macroconidia, and the only production of monophialides [17,42]. Molecular identification and discrimination were supported by the amplification of *tef-1α* and *rpb2* loci [17]. The identification of species belonging to FOSC represents a great challenge due to the complexity and the endless evolution of the taxonomy of the genus *Fusarium*. During the last decades, a plethora of new species was described, increasing problems for *Fusarium* taxonomy users [43]. Therefore, there is an agreement on the need to stabilize

 doi:10.20944/preprints202310.0504.v1

the taxonomy of the complex while conducting further studies to clarify species concepts to allow the correct characterization of species within FOSC. [17,43,44]. The high species diversity, found in the present study from a molecular point of view, should be supported by analyses on the pathogenicity and host preference of these species.

The pathogenicity tests, hereby performed, confirmed that all the species were able to cause symptoms of crown and root rot in maize seedlings. This is in line with the results obtained by other scientists which contribute to increase the knowledge on the complexity of the maize microbiome and on the etiology of soilborne diseases [45–47]. The isolates that were confirmed as pathogenic, showed different levels of aggressiveness on maize seedlings. The *F. verticillioides*, *F. annulatum*, *F. commune* isolates always showed a disease index higher than 50%, except for one isolate of *F. verticillioides* (8.2) that showed a disease index of 20%. Regarding the isolates belonging to FOSC, one isolate of *F. oxysporum sensu lato* and the isolate of *F. nirenbergiae* showed a disease index higher than 50%, while the other isolates of *F. oxysporum sensu lato* and the isolate of *F. cugenangense* showed lower indexes, ranging from 20% to 45%. Considering the economic and agronomic relevance of maize, and the susceptibility of this crop to pathogenic *Fusarium* species, it is important to provide a correct diagnosis for a rapid and effective disease management. This study investigated the species involved in maize diseases associated with symptoms of stalk, crown, and root rot in Northern Italy as well as those associated with seeds from different countries. Moreover, it provides useful information on tools to analyze the target loci to identify *Fusarium* species laying the base for future studies on their detection to develop specific and sensitive diagnostic tools that speed up the diagnosis of these pathogens. The identification process usually requires long time and several steps, starting from the description of the symptoms, the environmental conditions in which the infection occurred, the isolation, purification and morphological and molecular identification of the causal agents of the disease observed [48]. The development of rapid, specific and accurate molecular diagnostic tools could allow the identification and quantification of multiple pathogens in symptomatic plants and seeds as well as in those not yet expressing symptoms. Further investigations should be addressed to evaluate the putative cross pathogenicity of these species and the seed-borne rate in causing the symptoms observed in the field and reproduced in this study, to provide a deeper insight on the pathogens and disease development, then to improve management sustainable control strategies.

4. Materials and Methods

4.1. Fungal isolates

During 2019 and 2020, different surveys were conducted in six maize fields in Northern Italy. The surveyed fields were in San Zenone degli Ezzelini (VI), Cigliano (VC) and Crescentino (VC). Root and crown rot symptoms were detected on seedlings of different hybrids of maize early in the season, between V1 (first leaf) and V3 (third leaf) phenological stage. Symptomatic samples were collected and washed under running tap water for 2 minutes to remove soil debris. Small sections (0.1-0.2 cm) were cut on the edge of the symptomatic portions, surface sterilized in 1% hypochlorite solution for one min, rinsed in sterile distilled water and placed on potato dextrose agar (PDA, Merck, USA) to isolate fungi. After an incubation of 72 hours at room temperature, the plates were observed and mycelial plugs from the developed fungal colonies were transferred on new PDA plates to obtain pure cultures.

In 2019, from 24 commercial lots , produced in 5 different countries (France, Italy, Romania, Turkey and USA), 500 g of seeds were sampled and analysed with an incubation test to evaluate their phytosanitary conditions [49]. A total of 400 seeds of each lot was disinfected with 100 ml of a water solution containing 55.9% of commercial chlorine (5.37%), 10.4% of absolute alcohol (96%) and 10 µl of Tween 20 for 15 min and then rinsed three times with sterile distilled water and dried on sterile paper. The disinfected seeds were placed in 12 × 12 plastic boxes over three layers of sterile filter paper soaked with a 0.05% sodium hypochlorite water solution. The boxes were placed in a growth chamber at 25 °C ± 2 °C, under a 12 h near-ultraviolet light (NUV)12 h dark cycle, for 48 h, then for

 doi:10.20944/preprints202310.0504.v1

24 h at -20 °C and then incubated in the growth chamber for 11 days. Colonies were isolated from seeds and placed on PDA plates to obtain pure cultures.

4.2. Pathogenicity test

The pathogenicity of the 41 isolates was assessed following the protocol described by Okello et al. [15]. Pure cultures of the isolates were grown on PDA, amended with 25 mg/L of streptomycin sulphate, for 14 days at room temperature. After two weeks, mycelium plugs (15 mm) of each isolate were transferred into conical flasks (250 ml) containing a sterile sand/corn meal substrate, prepared with 54 g of sand, 6 g of corn meal and 10 ml of deionized water per flask. Five replicate flasks were used for each isolate. The inoculated flasks were then incubated at 23±2°C for 23 day, mixing them daily. A total of 300 maize seeds (P1565, Pioneer Hi-Bred, Italy) was incubated at 23±2°C for three days in Petri dishes filled with moisturized sterile filter paper to promote their germination and to obtain seedlings for inoculation. Once germinated, six seedlings per isolate were transplanted in inoculated pots (volume 2L) filled, following the protocol described by Bilgi et al. [50], with a first layer of 40 g of perlite, followed by a second layer of 20 g of inoculum and a final layer of 20 g of perlite. A total of 123 inoculated plastic pots were used considering 2 seedling per pot and 3 pots per fungal isolate. The pots were incubated in the greenhouse at 22±2°C for 14 days. The root rot severity was assessed with a scale that ranged from 1 to 5 at 14 days post-inoculation. The adopted scale was as follow: 1 = germinated seed and healthy seedling without symptoms of root rot; 2 = germinated seeds and 1-19% of symptomatic roots; 3 = germinated seed and 20-74% of symptomatic roots; 4 = germinated seed and> 75% symptomatic roots; 5 = complete colonization of the seed and undeveloped seedling [51]. The data were expressed as disease index (DI) 0–100, calculated with the following formula: DI= [$\sum$ (i × ni)]/(4 × total of plants)]×100; where i = 0–4 and ni is the number of plants with rating i. The assay was performed in triplicate and the data obtained expressed as mean value of the three replications carried out.

4.3. Data analyses

The data were subjected to analysis of variance (ANOVA), after testing that the resulting disease index data were normally distributed with a Levene's test, using SPSS Statistics v. 27.0 (IBM Corp., Armonk, NY, U.S.A.). The Duncan's test was used to explore differences between multiple group means ($p \leq 0.05$). Statistical analysis was performed with the Statistical Package for Social Science (SPSS, IBM, Chicago, IL, USA) version 27.0.

4.4. DNA extraction, PCR and sequencing

A total of 23 isolates was selected as representative based on their positive results in the pathogenicity test and used for the following analyses. Genomic DNA was extracted from each isolate, transferring 100 mg of mycelium in a 2 mL microcentrifuge tube and following the manufacturers' instructions of the Omega E.Z.N.A.® Fungal DNA mini kit (Omega Bio-Tek, Norcross, GA, USA), after a 15-min cycle, at 25 Hz, in Tissuelyser (Qiagen®). *Partial translation elongation factor-1α* (*tef-1α*), *RNA polymerase second largest subunit* (*rpb2*), *calmodulin* (*calm*), and *beta-tubulin* (*tub2*) genomic regions were amplified using EF1 and EF2 [52], rpb2-7cr and rpb2-5f [53], CAL-228f and CAL-737r [54], CL1 and CL2A [24] and T1 [55] and Bt2b [56] primers, respectively. The PCR mixtures and the cycling conditions for the amplification of *tef-1α*, *calm* and *tub2* followed the protocols described by Guarnaccia et al. [57] and Weir et al. [58]. For the *rpb2* the PCR protocol by Yilmaz et al. [16] was optimized as follows: 94 °C 90 s; 40 cycles of 94 °C 30 s, 55 °C 90 s, 68 °C 2 min; 68 °C 5 min. PCR amplification was checked by electrophoresis on 1% agarose (VWR Life Science AMRESCO® biochemicals) gels stained with GelRed™. PCR products were sequenced by BMR Genomics (Padova, Italy) and the obtained sequences were analyzed and assembled with the program Geneious v. 11.1.5 (Auckland, New Zealand).

 doi:10.20944/preprints202310.0504.v1

4.5. Phylogenetic analyses

The sequences generated in this research were analysed with the NCBIs GenBank database through the BLAST-N program to determine the closest species and the species complexes to which they belong and then compared with reference sequences reported in literature [16–19,24,39,44,59–66] and downloaded from GenBank, to establish the identity of the explored isolates. All the different regions of the sequences of this study and those downloaded from GenBank were aligned with the MAFFT v. 7 online server (http://mafft.cbrc.jp/alignment/server/index.html) [67], and then manually adjusted in MEGA v. 7 [68]. A preliminary analysis was conducted on the tef1-α region (data not shown) to determine which species complex the representative isolates belonged to. Phylogeny was processed through different analyses conducted as multilocus sequence analyses using different datasets in accordance with previous studies [16,17,19]. The analysis for the FFSC and the FNSC were performed combining *tef-1α*, *rpb2*, *calm* and *tub2* datasets, rooted with *F. foetens* (CBS 120665) and *F. udum* (NRRL 22949), respectively. The combined *tef-1α*, *rpb2* and *calm* datasets were used to perform the analyses for the FOSC, rooted with *F. udum* (NRRL 22949). The phylogenies were based on Maximum-Parsimony (MP) and Bayesian Inference (BI) methods. The MP analysis were performed with PAUP [69], while the Bayesian analyses were carried out with MrBayes v. 3.2.5 [70], including the best evolutionary model for each partition as defined by MrModelTest v. 2.3 [71]. BI analyses were processed using four Markov Chain Monte Carlo (MCMC) chains with a sampling frequency of 1000 generations. The heating condition was set to 0.2 and the analyses end when the standard deviation of split frequencies was less than 0.01. For the MP analyses, phylogenetic relationships were estimated by heuristic searches with 100 random addition sequences. Tree bisection-reconnection was used, with the branch swapping option set on 'best trees' only with all characters weighted equally and alignment gaps treated as fifth state. Tree length (TL), consistency index (CI), retention index (RI) and rescaled consistence index (RC) were calculated for parsimony and the bootstrap analyses were based on 1000 replications. The clade is supported when the Bootstrap support value is ≥ 70 %, and the Bayesian PP value is ≥ 0.9. Sequences generated and used in this study were deposited in GenBank (Table 3).

Table 3. Origin, host, culture and sequence GenBank accession number of *Fusarium* isolates used and generated in this study. Newly generated accession numbers are in bold.

Species	Complex	Collection	Host	Origin	*tef1-α*	*rpb2*	*calm*	*tub2*	Reference
F. acutatum	FFSC	CBS 401.97	*Cajanus cajan*	India	MW402124	MW402813	MW402458	MW402322	Yilmaz et al. (2021)
F. agapanthi	FFSC	CBS 100193	*Agapanthus praecox*	New Zealand	MW401959	MW402727	MW402363	MW402160	Yilmaz et al. (2021)
F. aglaonematis	FFSC	ZHKUCC 22-0079	*Aglaonema modestum*	China	ON330439	ON330445	ON330436	ON330442	Zhang et al. (2022)
F. ananatum	FFSC	CBS 118516	*Ananas comosus*	South Africa	LT996091	LT996137	MW402376	MN534089	Yilmaz et al. (2021)
F. andiyazi	FFSC	CBS 119856	Sorghum grain	Ethiopia	MN533989	MN534286	MN534174	MN534081	Yilmaz et al. (2021)
F. annulatum	FFSC	CBS 115.97	*Dianthus caryophyllus*	Italy	MW401973	MW402785	MW402373	MW402173	Yilmaz et al. (2021)
F. annulatum	FFSC	CBS 133.95	*Dianthus caryophyllus*	The Netherlands	MW402040	MW402743	MW402407	MW402239	Yilmaz et al. (2021)
F. annulatum	FFSC	CBS 135.95	*Dianthus caryophyllus*	The Netherlands	MW402043	MW402745	MW402408	MW402242	Yilmaz et al. (2021)
F. annulatum	FFSC	2.1	*Zea mays*	Italy	OR565982	OR566043	OR566020	OR566004	This study
F. annulatum	FFSC	2.2	*Zea mays*	Italy	OR565983	OR566044	OR566021	OR566005	This study
F. annulatum	FFSC	9	*Zea mays*	Italy	OR565984	OR566045	OR566022	OR566006	This study
F. annulatum	FFSC	10.1	*Zea mays*	Italy	OR565985	OR566046	OR566023	OR566007	This study
F. annulatum	FFSC	10.2	*Zea mays*	Italy	OR565986	OR566047	OR566024	OR566008	This study
F. annulatum	FFSC	55	*Zea mays*	Italy	OR565987	OR566048	OR566025	OR566009	This study
F. anthophilum	FFSC	CBS 108.92	*Hippeastrum* leaf	The Netherlands	MW401965	MW402783	MW402368	MW402166	Yilmaz et al. (2021)
F. aquaticum	FFSC	LC7502	Water	China	MW580448	MW474394	MW566275	MW533730	Wang (2022)
F. awaxy	FFSC	CBS 119831	Environmental	New Guinea	MN534056	MN534237	MN534167	MN534108	Yilmaz et al. (2021)
F. babinda	FFSC	NRRL 25539	Unknown	Unknown	KU171718	KU171698	KU171418	KU171778	O' Donnell et al. (2013)

doi:10.20944/preprints202310.0504.v1

F. bactridioides	FFSC	CBS 100057	*Cronartium conigenum* on *Pinus leiophylla*	USA	MN533993	MN534235	MN534173	MN534112	Yilmaz et al. (2021)
F. begoniae	FFSC	CBS 452.97	*Begonia elatior* hybrid	Germany	MN533994	MN534243	MN534163	MN534101	Yilmaz et al. (2021)
F. braichiariae	FFSC	CML 3163	*Brachiaria decumbens*	Brazil	MT901349	MT901315	-	MT901322	Moreira Costa et al. (2021)
F. brevicatenulatum	FFSC	CBS 404.97	*Striga asiatica*	Madagascar	MN533995	MN534295	MT010979	MN534063	Yilmaz et al. (2021)
F. bulbicola	FFSC	NRRL13618	*Nerine bowdenii* bulb	The Netherlands	KF466415	MW402767	MW402450	KF466437	Yilmaz et al. (2021)
F. caapi	FFSC	LLC3556	*Sorghum*	Ethiopia	OP486950	OP486519	OP485837	-	Lombard et al. (2022)
F. callistephi	FOSC	CBS 187.53	*Callistephus chinensis*	The Netherlands	MH484966	MH484875	MH484693	MH485057	Lombard et al. (2019)
F. carminascens	FOSC	CPC 25792	*Zea mays*	South Africa	MH485025	MH484934	MH484752	MH485116	Lombard et al. (2019)
F. casha	FFSC	PPRI20462	*Amaranthus cruentus*	South Africa	MF787262	-	-	MF787256	Vermeulen et al. (2021)
F. chinhoyiense	FFSC	NRRL 25221	*Zea mays*	Zimbabwe	MN534050	MN534262	MN534196	MN534082	Yilmaz et al. (2021)
F. chuoi	FFSC	CPC 39664	Unknown	Unknown	OK626308	OK626302	OK626304	OK626310	Yilmaz et al. (2021)
F. circinatum	FFSC	CBS 405.97	*Pinus radiata*	USA	MN533997	MN534252	MN534199	MN534097	Yilmaz et al. (2021)
F. coicis	FFSC	RBG5368	*Coix gasteenii*	Australia	KP083251	KP083274	LT996178	LT996115	Laurence et al. (2015)
F. commune	FNSC	NRRL 28387	*Dianthus caryophyllus*	The Netherlands	HM057338	JX171638	KU171420	AY329043	Han et al. (2023)
F. commune	FNSC	LC18507	*Zea mays*	China	OQ125095	OQ125101	-	-	Han et al. (2023)
F. commune	FNSC	LC18486	*Zea mays*	China	OQ125094	OQ125100	-	-	Han et al. (2023)
F. commune	FNSC	LC18652	*Zea mays*	China	OQ125093	OQ125099	-	-	Han et al. (2023)
F. commune	FNSC	LC18609	*Zea mays*	China	OQ125092	OQ125098	-	-	Han et al. (2023)
F. commune	FNSC	LC18583	*Zea mays*	China	OQ125097	OQ125103	-	-	Han et al. (2023)
F. commune	FNSC	LC18568	*Zea mays*	China	OQ125096	OQ125102	-	-	Han et al. (2023)
F. commune	FNSC	DB19LUG07	*Zea mays*	Italy	MW419921	MW419923	OR566042	OR566011	Mezzalama et al. (2021), This study

F. commune	FNSC	24	*Zea mays*	Italy	OR565988	OR566049	OR566026	OR566010	This study
F. concentricum	FFSC	CBS 450.97	*Musa sapientum*	Costa Rica	AF160282	JF741086	MW402467	MW402334	Yilmaz et al. (2021)
F. contaminatum	FOSC	CBS 111552	*Pasteurized fruit juice*	The Netherlands	MH484991	MH484900	MH484718	MH485082	Lombard et al. (2019)
F. cugenangense	FOSC	CBS 620.72	*Crocus* sp.	Germany	MH484970	MH484879	MH484697	MH485061	Lombard et al. (2019)
F. cugenangense	FOSC	CBS 130308	*Human toe nail*	New Zealand	MH485011	MH484920	MH484738	MH485102	Lombard et al. (2019)
F. cugenangense	FOSC	CBS 131393	*Vicia faba*	Australia	MH485019	MH484928	MH484746	MH485110	Lombard et al. (2019)
F. cugenangense	FOSC	CBS 130304	*Gossypium barbadense*	China	MH485012	MH484921	MH484739	MH485103	Lombard et al. (2019)
F. cugenangense	FOSC	36	*Zea mays*	Italy	OR565989	OR566050	OR566027	-	This study
F. curculicola	FFSC	PPRI20464	*Amaranthus cruentus*	South Africa	MF787267	MN605063	-	MF787259	Vermeulen et al. (2021)
F. curvatum	FOSC	CBS 247.61	*Matthiola incana*	Germany	MH484967	MH484876	MH484694	MH485058	Lombard et al. (2019)
F. curvatum	FOSC	CBS 238.94	*Beaucarnia* sp.	The Netherlands	MH484984	MH484893	MH484711	MH485075	Lombard et al. (2019)
F. curvatum	FOSC	CBS 141.95	*Hedera helix*	The Netherlands	MH484985	MH484894	MH484712	MH485076	Lombard et al. (2019)
F. denticulatum	FFSC	CBS 406.97	*Ipomoea batatas*	Cuba	MN533999	MN534273	MN534185	MN534067	Yilmaz et al. (2021)
F. dhileepanii	FFSC	BRIP 71717	Unknown	Unknown	OK509072	OK533536	-	-	Yilmaz et al. (2021)
F. dlaminii	FFSC	CBS 481.94	Unknown	Unknown	MN534003	MN534257	MN534151	MN534139	Yilmaz et al. (2021)
F. dlaminii	FFSC	CBS 671.94	Soil	South Africa	MN534004	MN534254	MN534152	MN534136	Yilmaz et al. (2021)
F. duoseptatum	FOSC	CBS 102026	*Musa sapientum*	Malaysia	MH484987	MH484896	MH484714	MH485078	Lombard et al. (2019)
F. echinatum	FFSC	CBS 146497	Unidentified tree	South Africa	MW834273	MW834004	MW834110	MW834301	Crous et al. (2021)
F. elaeagni	FFSC	LC13629	*Elaeagnus pungens*	China	MW580468	MW474414	MW566295	MW533750	Wang (2022)
F. elaeidis	FOSC	CBS 217.49	*Elaeis* sp.	Zaire	MH484961	MH484870	MH484688	MH485052	Lombard et al. (2019)
F. elaeidis	FOSC	CBS 255.52	*Elaeis guineensis*	Unknown	MH484965	MH484874	MH484692	MH485056	Lombard et al. (2019)
F. elaeidis	FOSC	CBS 218.49	*Elaeis sp.*	Zaire	MH484962	MH484871	MH484689	MH485053	Lombard et al. (2019)
F. fabacearum	FOSC	CPC 25801	*Zea mays*	South Africa	MH485029	MH484938	MH484756	MH485120	Lombard et al. (2019)
F. fabacearum	FOSC	CPC 25802	*Glycine max*	South Africa	MH485030	MH484939	MH484757	MH485121	Lombard et al. (2019)

F. fabacearum	FOSC	CPC 25803	*Glycine max*	South Africa	MH485031	MH484940	MH484758	MH485122	Lombard et al. (2019)
F. ficicrescens	FFSC	CBS 125177	Environmental	Iran	MN534006	MN534281	MN534176	MN534071	Yilmaz et al. (2021)
F. foetens	FOSC	CBS 120665	*Nicotiana tabacum*	Iran	MH485009	MH484918	MH484736	MH485100	Lombard et al. (2019)
F. fracticaudum	FFSC	CMW:25240	*Pinus maximinoi*	Colombia	MN534009	MN534231	MN534161	MN534103	Yilmaz et al. (2021)
F. fractiflexum	FFSC	NRRL 28852	*Cymbidium* sp.	Japan	AF160288	LT575064	AF158341	AF160315	Yilmaz et al. (2021)
F. fredkrugeri	FFSC	CBS 408.97	Soil	Maryland	MW402126	MW402814	MW402461	MW402324	Yilmaz et al. (2021)
F. fujikuroi	FFSC	CBS 186.56	Unknown	Unknown	MW402108	EF470116	MW402447	MW402306	Yilmaz et al. (2021)
F. gaditjirri	FNSC	NRRL 45417	*Hetepogon triticeus*	Australia	MN193881	MN193909	KU171424	KU171784	Sandoval-Denis et al. (2018)
F. globosum	FFSC	CBS 430.97	*Zea mays* seed	South Africa	MN534013	MN534265	MN534219	MN534125	Yilmaz et al. (2021)
F. glycines	FOSC	CBS 176.33	*Linum usitatissium*	Unknown	MH484959	MH484868	MH484686	MH485050	Lombard et al. (2019)
F. gossypinum	FOSC	CBS 116611	*Gossypium hirsutum*	Ivory Coast	MH484998	MH484907	MH484725	MH485089	Lombard et al. (2019)
F. gossypinum	FOSC	CBS 116613	*Gossypium hirsutum*	Ivory Coast	MH485000	MH484909	MH484727	MH485091	Lombard et al. (2019)
F. gossypinum	FOSC	CBS 116612	*Gossypium hirsutum*	Ivory Coast	MH484999	MH484908	MH484726	MH485090	Lombard et al. (2019)
F. guttiforme	FFSC	CBS 409.97	*Ananas comosus*	Brazil	MT010999	MT010967	MT010901	MT011048	Yilmaz et al. (2021)
F. hechiense	FFSC	LC13646	*Musa nana*	China	MW580496	MW474442	MW566323	MW533775	Wang (2022)
F. hoodiae	FOSC	CBS 132474	*Hoodia gordonii*	South Africa	MH485020	MH484929	MH484747	MH485111	Lombard et al. (2019)
F. inflexum	FOSC	NRRL 20433	*Vicia faba*	Germany	AF008479	JX171583	AF158366	–	O'Donnell et al. (2013)
F. konzum	FFSC	CBS 139382	Unknown	Unknown	MW402071	MW402804	MW402418	MW402270	Yilmaz et al. (2021)
F. lactis	FFSC	CBS 420.97	*Ficus carica*	USA	MN534015	-	MN534181	MN534078	Yilmaz et al. (2021)
F. languescens	FOSC	CBS 645.78	*Solanum lycopersicum*	Morocco	MH484971	MH484880	MH484698	MH485062	Lombard et al. (2019)
F. libertatis	FOSC	CPC 25782	*Asphalatus* sp.	South Africa	MH485023	MH484932	MH484750	MH485114	Lombard et al. (2019)
F. lumajangense	FFSC	LC13652	*Arenga caudata*	China	MW580503	MW474449	MW566330	MW533782	Wang (2022)
F. lyarnte	FNSC	NRRL 54252	*Sorghum interjectum*	Australia	MN193880	MN193908	-	-	Sandoval-Denis et al. (2018)
F. madaense	FFSC	CBS 146648	*Arachis hypogaea*	Nigeria	MW402095	MW402761	MW402436	MW402294	Yilmaz et al. (2021)
F. mangiferae	FFSC	CBS 119853	*Mangifera* sp.	South Africa	MN534016	MN534270	MN534225	MN534140	Yilmaz et al. (2021)

doi:10.20944/preprints202310.0504.v1

F. marasasianum	FFSC	CMW:25512	*Pinus tecunumanii*	Colombia	MN534018	MN534249	MN534208	MN534113	Yilmaz et al. (2021)
F. mexicanum	FFSC	NRRL 47473	*Mangifera indica*	Mexico	GU737416	LR792615	GU737389	GU737308	Yilmaz et al. (2021)
F. mirum	FFSC	LLC929	*Sorghum*	Ethiopia	OP487012	OP486581	OP485896	-	Lombard et al. (2022)
F. miscanthi	FNSC	NRRL 26231	*Miscanthus sinensis*	Japan	KU171725	KU171705	KU171425	KU171785	Han et al. (2023)
F. mundagurra	FFSC	RBG5717	Soil	Australia	KP083256	KP083276	MN534214	MN534146	Yilmaz et al. (2021)
F. napiforme	FFSC	NRRL25196	*Pennisetum typhoides*	South Africa	MN193863	MN534291	MN534192	MN534085	Laraba et al. (2020)
F. nirenbergiae	FOSC	CBS 129.24	*Secale cereale*	Unknown	MH484955	MH484864	MH484682	MH485046	Lombard et al. (2019)
F. nirenbergiae	FOSC	CBS 127.81	*Chrysantemum* sp.	USA	MH484974	MH484883	MH484701	MH485065	Lombard et al. (2019)
F. nirenbergiae	FOSC	CBS 840.88	*Dianthus caryophyllus*	The Netherlands	MH484978	MH484887	MH484705	MH485069	Lombard et al. (2019)
F. nirenbergiae	FOSC	CBS 744.79	*Passiflora edulis*	Brazil	MH484973	MH484882	MH484700	MH485064	Lombard et al. (2019)
F. nirenbergiae	FOSC	1RI (Pta 1.2)	*Zea mays*	Italy	OR565990	OR566051	OR566028	-	This study
F. nisikadoi	FNSC	NRRL 25179	*Phyllostachys nigra*	Japan	MN193879	MN193907	-	-	Sandoval-Denis et al. (2018)
F. nygamai	FFSC	CBS 413.97	*Oryza sativa*	Morocco	MW402127	MW402815	MW402462	MW402325	Yilmaz et al. (2021)
F. odoratissimum	FOSC	CBS 794.70	*Albizzia julibrissin*	Iran	MH484969	MH484878	MH484696	MH485060	Lombard et al. (2019)
F. ophioides	FFSC	CBS 118510	*Panicum maximum*	South Africa	MN534020	MN534301	MN534201	MN534121	Yilmaz et al. (2021)
F. oxysporum	FOSC	CBS 144134	*Solanum tuberosum*	Germany	MH485044	MH484953	MH484771	MH485135	Lombard et al. (2019)
F. oxysporum	FOSC	CBS 144135	*Solanum tuberosum*	Germany	MH485045	MH484954	MH484772	MH485136	Lombard et al. (2019)
F. oxysporum	FOSC	CBS 221.49	*Camellia sinensis*	South East Asia	MH484963	MH484872	MH484690	MH485054	Lombard et al. (2019)
F. oxysporum	FOSC	CPC 25822	*Protea* sp.	South Africa	MH485034	MH484943	MH484761	MH485125	Lombard et al. (2019)
F. oxysporum sensu lato	FOSC	11	*Zea mays*	Italy	OR565991	OR566052	OR566029	-	This study
F. oxysporum sensu lato	FOSC	12	*Zea mays*	Italy	OR565992	OR566053	OR566030	-	This study
F. oxysporum sensu lato	FOSC	18	*Zea mays*	Italy	OR565993	OR566054	OR566031	-	This study

doi:10.20944/preprints202310.0504.v1

F. oxysporum sensu lato	FOSC	26	*Zea mays*	Italy	OR565994	OR566055	OR566032	-	This study
F. oxysporum sensu lato	FOSC	51	*Zea mays*	Italy	OR565995	OR566056	OR566033	-	This study
F. panlongense	FFSC	LC13656	*Musa nana*	China	MW580510	MW474456	MW566337	MW533789	Wang (2022)
F. paranisikadoi	FNSC	LC2824	*Zea mays*	China	MW594317	MW474550	-	MW533921	Han et al. (2023)
F. parvisorum	FFSC	CMW:25267	*Pinus patula*	Colombia	KJ541060	-	-	KJ541055	Yilmaz et al. (2021)
F. pharetrum	FOSC	CPC 30822	*Aliodendron dichotomum*	South Africa	MH485042	MH484951	MH484769	MH485133	Lombard et al. (2019)
F. phyllophilum	FFSC	NRRL13617	*Dracaena deremensis*	Italy	MN193864	KF466410	KF466333	KF466443	Laraba et al. (2020)
F. pilosicola	FFSC	NRRL 29123	*Bidens pilosa*	USA	MN534054	MN534247	MN534165	MN534098	Yilmaz et al. (2021)
F. pininemorale	FFSC	CMW:25243	*Pinus tecunumanii*	Colombia	MN534026	MN534250	MN534211	MN534115	Yilmaz et al. (2021)
F. proliferatum	FFSC	CBS 480.96	Tropical rain forest soil	Papua New Guinea	MN534059	MN534272	MN534217	MN534129	Yilmaz et al. (2021)
F. pseudoanthophilum	FFSC	CBS 745.97	*Zea mays*	Zimbabwe	MW402148	MW402820	MW402476	MW402349	Yilmaz et al. (2021)
F. pseudocircinatum	FFSC	NRRL22946	*Solanum* sp.	Ghana	AF160271	MN534277	MN534190	MN534069	O' Donnell et al. (2000)
F. pseudonygamai	FFSC	CBS 416.97	*Pennisetum typhoides*	Nigeria	MN534030	MN534283	MN534194	MN534064	Yilmaz et al. (2021)
F. ramigenum	FFSC	NRRL25208	*Ficus carica*	USA	KF466423	KF466412	MN534187	MN534145	Proctor et al. (2013)
F. sacchari	FFSC	CBS 131370	*Oryzae australiensis*	Australia	MW402031	MW402793	MW402404	MW402230	Yilmaz et al. (2021)
F. secorum	FFSC	NRRL 62593	*Beta vulgaris*	USA	KJ189225	–	KJ189235	–	Yilmaz et al. (2021)
F. siculi	FFSC	CPC 27188	*Citrus sinensis*	Italy	LT746214	LT746327	LT746189	LT746346	Sandoval-Denis et al. (2018)
F. sororula	FFSC	CMW:25513	*Pinus tecunumanii*	Colombia	MN534035	MN534246	MN534210	MN534114	Yilmaz et al. (2021)
F. sterilihyposum	FFSC	NRRL 25623	*Mangifera sp.*	South Africa	MN193869	MN193897	AF158353	AF160316	Yilmaz et al. (2021)
F. subglutinans	FFSC	CBS 215.76	*Zea mays*	Germany	MN534061	MN534241	MN534171	MN534109	Yilmaz et al. (2021)
F. succisae	FFSC	CBS 187.34	*Zostera marina*	UK	MW402109	MW402810	MW402448	MW402307	Yilmaz et al. (2021)
F. sudanense	FFSC	CBS 454.97	*Striga hermonthica*	Sudan	MN534037	MN534278	MN534179	MN534073	Yilmaz et al. (2021)

F. tardichlamydosporum	FOSC	CBS 102028	*Musa sapientum*	Malaysia	MH484988	MH484897	MH484715	MH485079	Lombard et al. (2019)
F. temperatum	FFSC	CBS 135538	Pulmonary infection (human)	Mexico	MN534039	MN534239	MN534168	MN534111	Yilmaz et al. (2021)
F. terricola	FFSC	CBS 483.94	Soil	Australia	MN534042	LT996156	MN534189	MN534076	Yilmaz et al. (2021)
F. thapsinum	FFSC	CBS 539.79	Man, white grained mycetoma	Italy	MW402140	MW402818	MW402472	MW402340	Yilmaz et al. (2021)
F. tjaetaba	FFSC	RBG5361	*Sorghum interjectum*	Australia	KP083263	KP083275	LT996187	GU737296	Laurence et al. (2015)
F. triseptatum	FOSC	CBS 258.50	*Ipomoea batatas*	USA	MH484964	MH484873	MH484691	MH485055	Lombard et al. (2019)
F. tupiense	FFSC	NRRL 53984	*Mangifera indica*	Brazil	GU737404	LR792619	GU737377	GU737350	Yilmaz et al. (2021)
F. udum	FFSC	NRRL22949	Unknown	Unknown	AF160275	LT996172	MW402442	U34433	O' Donnell et al. (2000)
F. verticillioides	FFSC	CBS 116665	*Solanum lycopersicum*	Unknown	MW401976	MW402825	MW402375	MW402176	Yilmaz et al. (2021)
F. verticillioides	FFSC	CBS 125.73	*Trichosanthes dioica*	India	MW402012	MW402791	MW402392	MW402212	Yilmaz et al. (2021)
F. verticillioides	FFSC	CBS 167.87	*Pinus* seed	USA	MW402101	-	MW402441	MW402300	Yilmaz et al. (2021)
F. verticillioides	FFSC	CBS 447.95	*Asparagus*	Unknown	MW402133	MW402770	MW402466	MW402332	Yilmaz et al. (2021)
F. verticillioides	FFSC	CBS 531.95	*Zea mays*	Unknown	MW402136	MW402771	MW402468	MW402336	Yilmaz et al. (2021)
F. verticillioides	FFSC	CBS 131389	Environmental	Australia	KU711695	KU604226	MN534193	KU603857	Yilmaz et al. (2021)
F. verticillioides	FFSC	CBS 734.97	*Zea mays*	Germany	MW402146	EF470122	AF158315	MW402346	Yilmaz et al. (2021)
F. verticillioides	FFSC	8.2	*Zea mays*	Italy	OR565996	OR566057	OR566034	OR566012	This study
F. verticillioides	FFSC	35.1.4	*Zea mays*	Italy	OR565997	OR566058	OR566035	OR566013	This study
F. verticillioides	FFSC	56.1.2	*Zea mays*	Italy	OR565998	OR566059	OR566036	OR566014	This study
F. verticillioides	FFSC	56.2.2	*Zea mays*	Italy	OR565999	OR566060	OR566037	OR566015	This study
F. verticillioides	FFSC	56.2.3	*Zea mays*	Italy	OR566000	OR566061	OR566038	OR566016	This study
F. verticillioides	FFSC	56.2.4	*Zea mays*	Italy	OR566001	OR566062	OR566039	OR566017	This study
F. verticillioides	FFSC	56.2.5	*Zea mays*	Italy	OR566002	OR566063	OR566040	OR566018	This study
F. verticillioides	FFSC	57.2.1	*Zea mays*	Italy	OR566003	OR566064	OR566041	OR566019	This study

doi:10.20944/preprints202310.0504.v1

F. veterinarium	FOSC	CBS 109898	*Shark peritoneum*	The Netherlands	MH484990	MH484899	MH484717	MH485081	Lombard et al. (2019)
F. volatile	FFSC	CBS 143874	Human bronchoalveolar lavage fluid	French Guiana	LR596007	LR596006	MK984595	LR596008	Yilmaz et al. (2021)
F. werrikimbe	FFSC	CBS 125535	*Sorghum leiocladum*	Australia	MW928846	MN534304	MN534203	MN534104	Yilmaz et al. (2021)
F. xylarioides	FFSC	NRRL25486	*Coffea* trunk	Ivory Coast	MN193874	HM068355	MW402455	AY707118	Laraba et al. (2020)
F. xyrophilum	FFSC	NRRL 62710	*Xyris* spp.	Guyana	MN193875	MN193903	–	–	Yilmaz et al. (2021)

doi:10.20944/preprints202310.0504.v1

 doi:10.20944/preprints202310.0504.v1

4.6. Morphology

The characterization and the description of *Fusarium* isolates was conducted using macro and micromorphological features as described by Leslie et al. [25]. Single conidia colonies of the 23 representative isolates were grown on PDA for 10 days. Colony growth and macromorphological features were determined by placing agar plugs (5 mm), taken from the edge of actively growing cultures, on PDA plates incubated at 25±1°C, under a 12/12 h near UV light, for 7 days [66]. All the isolates were transferred on carnation leaf agar (CLA) plates [72], and incubated at 25±1°C under a 12/12h near UV light for 14 days to induce sporulation. Micromorphological features were observed and 50 random measurements of macroconidia, microconidia, conidiogenous cells and chlamydospores were done for each isolate at 40X magnification with a Leica DM2500 microscope. The observations were made by placing the plates directly under the microscope. Measurements were reported as mean value, standard deviation, minimum, and maximum values.

Author Contributions: Conceptualization, M.M and M.S.; methodology, M.S.; formal analysis, M.S. V.G. I.M.; resources, M.M.; data curation, M.S. I.M.; writing—original draft preparation, M.S.; writing—review and editing, M.S. M.M. I.M. V.G..; supervision, M.M., V.G.; funding acquisition, M.M.

Funding: This research was funded by AGROINNOVA DIAGNOSTICS Laboratory. www.agroinnova.unito.it

Data Availability Statement: Not applicable.

Acknowledgments: Authors thank CAPAC Soc. Coop. Agricola, Torino, Italy for providing the seed samples and dr. Marco Troisi, CORTEVA Agriscience, Italy, for providing the maize seedlings.

Conflicts of Interest: The authors declare no conflict of interest.

References

1. Erenstein, O.; Jaleta, M.; Sonder, K.; Mottaleb, K.; Prasanna, B. M. Global Maize Production, Consumption and Trade: Trends and R&D Implications. *Food Secur.* **2022**, *14* (5), 1295–1319. https://doi.org/10.1007/s12571-022-01288-7.
2. *FAOSTAT*. https://www.fao.org/faostat/en/%3F%23data#data/QCL/visualize (accessed 2023-07-21).
3. *Coltivazioni : Cereali, legumi, radici bulbi e tuberi*. http://dati.istat.it/Index.aspx?QueryId=33702 (accessed 2023-07-21).
4. Munkvold, G.; White, D. *Compendium of Corn Diseases.*; AACC International, 2016.
5. Ma, L.-J.; Geiser, D. M.; Proctor, R. H.; Rooney, A. P.; O'Donnell, K.; Trail, F.; Gardiner, D. M.; Manners, J. M.; Kazan, K. Fusarium Pathogenomics. *Annu. Rev. Microbiol.* **2013**, *67*, 399–416.
6. Oldenburg, E.; Höppner, F.; Ellner, F.; Weinert, J. Fusarium Diseases of Maize Associated with Mycotoxin Contamination of Agricultural Products Intended to Be Used for Food and Feed. *Mycotoxin Res.* **2017**, *33* (3), 167–182.
7. Logrieco, A.; Bottalico, A.; Mulé, G.; Moretti, A.; Perrone, G. Epidemiology of Toxigenic Fungi and Their Associated Mycotoxins for Some Mediterranean Crops. *Epidemiol. Mycotoxin Prod. Fungi Aegis COST Action 835 'Agriculturally Important Toxigenic Fungi 1998–2003' EU Proj. QLK 1-CT-1998–01380* **2003**, 645–667.
8. Zargaryan, N. Y.; Kekalo, A. Y.; Nemchenko, V. V. Infection of Grain Crops with Fungi of the Genus Fusarium. In *BIO Web of Conferences*; EDP Sciences, 2021; Vol. 36, p 04008.
9. Desjardins, A. E. *Fusarium Mycotoxins: Chemistry, Genetics, and Biology.*; American Phytopathological Society (APS Press), 2006.
10. Leyva-Madrigal, K. Y.; Larralde-Corona, C. P.; Apodaca-Sánchez, M. A.; Quiroz-Figueroa, F. R.; Mexia-Bolaños, P. A.; Portillo-Valenzuela, S.; Ordaz-Ochoa, J.; Maldonado-Mendoza, I. E. Fusarium Species from the Fusarium Fujikuroi Species Complex Involved in Mixed Infections of Maize in Northern Sinaloa, Mexico. *J. Phytopathol.* **2015**, *163* (6), 486–497.
11. Duan, C.; Qin, Z.; Yang, Z.; Li, W.; Sun, S.; Zhu, Z.; Wang, X. Identification of Pathogenic Fusarium Spp. Causing Maize Ear Rot and Potential Mycotoxin Production in China. *Toxins* **2016**, *8* (6), 186.
12. Wilke, A. L.; Bronson, C. R.; Tomas, A.; Munkvold, G. P. Seed Transmission of Fusarium Verticillioides in Maize Plants Grown under Three Different Temperature Regimes. *Plant Dis.* **2007**, *91* (9), 1109–1115.

13. Kedera, C. J.; Leslie, J. F.; Claflin, L. E. Systemic Infection of Corn by Fusarium Moniliforme. *Phytopathology* **1992**, *82*, 1138.
14. Munkvold, G. P.; McGee, D. C.; Carlton, W. M. Importance of Different Pathways for Maize Kernel Infection by Fusarium Moniliforme. *Phytopathology* **1997**, *87* (2), 209–217.
15. Okello, P. N.; Petrović, K.; Kontz, B.; Mathew, F. M. Eight Species of Fusarium Cause Root Rot of Corn (Zea Mays) in South Dakota. *Plant Health Prog.* **2019**, *20* (1), 38–43.
16. Yilmaz, N.; Sandoval-Denis, M.; Lombard, L.; Visagie, C. M.; Wingfield, B. D.; Crous, P. W. Redefining Species Limits in the Fusarium Fujikuroi Species Complex. *Persoonia-Mol. Phylogeny Evol. Fungi* **2021**, *46* (1), 129–162.
17. Lombard, L.; Sandoval-Denis, M.; Lamprecht, S. C.; Crous, P. W. Epitypification of Fusarium Oxysporum–Clearing the Taxonomic Chaos. *Persoonia-Mol. Phylogeny Evol. Fungi* **2019**, *43* (1), 1–47.
18. Wang, M. M.; Crous, P. W.; Sandoval-Denis, M.; Han, S. L.; Liu, F.; Liang, J. M.; Duan, W. J.; Cai, L. Fusarium and Allied Genera from China: Species Diversity and Distribution. *Persoonia-Mol. Phylogeny Evol. Fungi* **2022**, *48* (1), 1–53.
19. Han, S. L.; Wang, M. M.; Ma, Z. Y.; Raza, M.; Zhao, P.; Liang, J. M.; Gao, M.; Li, Y. J.; Wang, J. W.; Hu, D. M. Fusarium Diversity Associated with Diseased Cereals in China, with an Updated Phylogenomic Assessment of the Genus. *Stud. Mycol.* **2023**.
20. Geiser, D. M.; del Mar Jiménez-Gasco, M.; Kang, S.; Makalowska, I.; Veeraraghavan, N.; Ward, T. J.; Zhang, N.; Kuldau, G. A.; O'donnell, K. FUSARIUM-ID v. 1.0: A DNA Sequence Database for Identifying Fusarium. *Eur. J. Plant Pathol.* **2004**, *110*, 473–479.
21. O'Donnell, K.; Ward, T. J.; Robert, V. A.; Crous, P. W.; Geiser, D. M.; Kang, S. DNA Sequence-Based Identification of Fusarium: Current Status and Future Directions. *Phytoparasitica* **2015**, *43*, 583–595.
22. O'Donnell, K.; Whitaker, B. K.; Laraba, I.; Proctor, R. H.; Brown, D. W.; Broders, K.; Kim, H.-S.; McCormick, S. P.; Busman, M.; Aoki, T. DNA Sequence-Based Identification of Fusarium: A Work in Progress. *Plant Dis.* **2022**, *106* (6), 1597–1609.
23. Leslie, J. F. Introductory Biology of Fusarium Moniliforme. In *Fumonisins in Food*; Jackson, L. S., DeVries, J. W., Bullerman, L. B., Eds.; Advances in Experimental medicine and Biology; Springer US: Boston, MA, 1996; pp 153–164. https://doi.org/10.1007/978-1-4899-1379-1_14.
24. O'Donnell, K.; Nirenberg, H. I.; Aoki, T.; Cigelnik, E. A Multigene Phylogeny of the Gibberella Fujikuroi Species Complex: Detection of Additional Phylogenetically Distinct Species. *Mycoscience* **2000**, *41* (1), 61–78. https://doi.org/10.1007/BF02464387.
25. Leslie, J. F.; Summerell, B. A. *The Fusarium Laboratory Manual*; John Wiley & Sons, 2008.
26. Murillo-Williams, A.; Munkvold, G. P. Systemic Infection by Fusarium Verticillioides in Maize Plants Grown Under Three Temperature Regimes. *Plant Dis.* **2008**, *92* (12), 1695–1700. https://doi.org/10.1094/PDIS-92-12-1695.
27. Nezhad, A. S.; Nourollahi, K. Population Genetic Structure of Fusarium Verticillioides the Causal Agent of Corn Crown and Root Rot in Ilam Province Using Microsatellite Markers. *J. Crop Prot.* **2020**, *9* (1), 157–170.
28. Bugnicourt, F. Une Espèce Fusarienne Nouvelle, Parasite Du Riz. *Rev. Génerale Bot.* **1952**, *59*, 13–18.
29. PARRA, M. Ä.; Gómez, J.; Aguilar, F. W.; Martínez, J. A. Fusarium Annulatum Causes Fusarium Rot of Cantaloupe Melons in Spain. *Phytopathol. Mediterr.* **2022**, *61* (2), 269–277.
30. Mirghasempour, S. A.; Studholme, D. J.; Chen, W.; Cui, D.; Mao, B. Identification and Characterization of Fusarium Nirenbergiae Associated with Saffron Corm Rot Disease. *Plant Dis.* **2022**, *106* (2), 486–495. https://doi.org/10.1094/PDIS-04-21-0871-RE.
31. Özer, G.; Paulitz, T. C.; Imren, M.; Alkan, M.; Muminjanov, H.; Dababat, A. A. Identity and Pathogenicity of Fungi Associated with Crown and Root Rot of Dryland Winter Wheat in Azerbaijan. *Plant Dis.* **2020**, *104* (8), 2149–2157. https://doi.org/10.1094/PDIS-08-19-1799-RE.
32. O'Donnell, K.; Cigelnik, E.; Nirenberg, H. I. Molecular Systematics and Phylogeography of the *Gibberella Fujikuroi* Species Complex. *Mycologia* **1998**, *90* (3), 465–493. https://doi.org/10.1080/00275514.1998.12026933.
33. Wulff, E. G.; Sørensen, J. L.; Lübeck, M.; Nielsen, K. F.; Thrane, U.; Torp, J. Fusarium Spp. Associated with Rice Bakanae: Ecology, Genetic Diversity, Pathogenicity and Toxigenicity. *Environ. Microbiol.* **2010**, *12* (3), 649–657. https://doi.org/10.1111/j.1462-2920.2009.02105.x.
34. Husna, A.; Zakaria, L.; Nor, N. M. I. M. Fusarium Commune Associated with Wilt and Root Rot Disease in Rice. *Plant Pathol.* **2020**, *70* (1), 123–132.

35. Mezzalama, M.; Guarnaccia, V.; Martino, I.; Tabone, G.; Gullino, M. L. First Report of Fusarium Commune Causing Root and Crown Rot on Maize in Italy. *Plant Dis.* **2021**, *105* (12), 4156. https://doi.org/10.1094/PDIS-01-21-0075-PDN.
36. Xi, K.; Haseeb, H. A.; Shan, L.; Guo, W.; Dai, X. First Report of Fusarium Commune Causing Stalk Rot on Maize in Liaoning Province, China. *Plant Dis.* **2019**, *103* (4), 773–773. https://doi.org/10.1094/PDIS-09-18-1674-PDN.
37. Skovgaard, K.; Rosendahl, S.; O'Donnell, K.; Nirenberg, H. I. Fusarium Commune Is a New Species Identified by Morphological and Molecular Phylogenetic Data. *Mycologia* **2003**, *95* (4), 630–636.
38. Dean, R.; Van Kan, J. A.; Pretorius, Z. A.; Hammond-Kosack, K. E.; Di Pietro, A.; Spanu, P. D.; Rudd, J. J.; Dickman, M.; Kahmann, R.; Ellis, J. The Top 10 Fungal Pathogens in Molecular Plant Pathology. *Mol. Plant Pathol.* **2012**, *13* (4), 414–430.
39. Laurence, M.; Walsh, J. L.; Shuttleworth, L.; Robinson, D. M.; Johansen, R. M.; Petrovic, T.; Vu, H.; Burgess, L. W.; Summerell, B.; Liew, E. C. Y. Six Novel Species of Fusarium from Natural Ecosystems in Australia. *Fungal Divers.* **2015**, *77*. https://doi.org/10.1007/s13225-015-0337-6.
40. Maymon, M.; Sharma, G.; Hazanovsky, M.; Erlich, O.; Pessach, S.; Freeman, S.; Tsror, L. Characterization of Fusarium Population Associated with Wilt of Jojoba in Israel. *Plant Pathol.* **2021**, *70*. https://doi.org/10.1111/ppa.13345.
41. Aiello, D.; Fiorenza, A.; Leonardi, G. R.; Vitale, A.; Polizzi, G. Fusarium Nirenbergiae (Fusarium Oxysporum Species Complex) Causing the Wilting of Passion Fruit in Italy. *Plants* **2021**, *10* (10), 2011.
42. Maryani, N.; Lombard, L.; Poerba, Y. S.; Subandiyah, S.; Crous, P. W.; Kema, G. H. J. Phylogeny and Genetic Diversity of the Banana Fusarium Wilt Pathogen Fusarium Oxysporum f. Sp. Cubense in the Indonesian Centre of Origin. *Stud. Mycol.* **2019**, *92*, 155–194. https://doi.org/10.1016/j.simyco.2018.06.003.
43. Summerell, B. A. Resolving Fusarium: Current Status of the Genus. *Annu. Rev. Phytopathol.* **2019**, *57* (1), 323–339. https://doi.org/10.1146/annurev-phyto-082718-100204.
44. Crous, P. W.; Lombard, L.; Sandoval-Denis, M.; Seifert, K. A.; Schroers, H.-J.; Chaverri, P.; Gené, J.; Guarro, J.; Hirooka, Y.; Bensch, K.; Kema, G. H. J.; Lamprecht, S. C.; Cai, L.; Rossman, A. Y.; Stadler, M.; Summerbell, R. C.; Taylor, J. W.; Ploch, S.; Visagie, C. M.; Yilmaz, N.; Frisvad, J. C.; Abdel-Azeem, A. M.; Abdollahzadeh, J.; Abdolrasouli, A.; Akulov, A.; Alberts, J. F.; Araújo, J. P. M.; Ariyawansa, H. A.; Bakhshi, M.; Bendiksby, M.; Ben Hadj Amor, A.; Bezerra, J. D. P.; Boekhout, T.; Câmara, M. P. S.; Carbia, M.; Cardinali, G.; Castañeda-Ruiz, R. F.; Celis, A.; Chaturvedi, V.; Collemare, J.; Croll, D.; Damm, U.; Decock, C. A.; de Vries, R. P.; Ezekiel, C. N.; Fan, X. L.; Fernández, N. B.; Gaya, E.; González, C. D.; Gramaje, D.; Groenewald, J. Z.; Grube, M.; Guevara-Suarez, M.; Gupta, V. K.; Guarnaccia, V.; Haddaji, A.; Hagen, F.; Haelewaters, D.; Hansen, K.; Hashimoto, A.; Hernández-Restrepo, M.; Houbraken, J.; Hubka, V.; Hyde, K. D.; Iturriaga, T.; Jeewon, R.; Johnston, P. R.; Jurjević, Ž.; Karalti, İ.; Korsten, L.; Kuramae, E. E.; Kušan, I.; Labuda, R.; Lawrence, D. P.; Lee, H. B.; Lechat, C.; Li, H. Y.; Litovka, Y. A.; Maharachchikumbura, S. S. N.; Marin-Felix, Y.; Matio Kemkuignou, B.; Matočec, N.; McTaggart, A. R.; Mlčoch, P.; Mugnai, L.; Nakashima, C.; Nilsson, R. H.; Noumeur, S. R.; Pavlov, I. N.; Peralta, M. P.; Phillips, A. J. L.; Pitt, J. I.; Polizzi, G.; Quaedvlieg, W.; Rajeshkumar, K. C.; Restrepo, S.; Rhaiem, A.; Robert, J.; Robert, V.; Rodrigues, A. M.; Salgado-Salazar, C.; Samson, R. A.; Santos, A. C. S.; Shivas, R. G.; Souza-Motta, C. M.; Sun, G. Y.; Swart, W. J.; Szoke, S.; Tan, Y. P.; Taylor, J. E.; Taylor, P. W. J.; Tiago, P. V.; Váczy, K. Z.; van de Wiele, N.; van der Merwe, N. A.; Verkley, G. J. M.; Vieira, W. A. S.; Vizzini, A.; Weir, B. S.; Wijayawardene, N. N.; Xia, J. W.; Yáñez-Morales, M. J.; Yurkov, A.; Zamora, J. C.; Zare, R.; Zhang, C. L.; Thines, M. Fusarium: More than a Node or a Foot-Shaped Basal Cell. *Stud. Mycol.* **2021**, *98*, 100116. https://doi.org/10.1016/j.simyco.2021.100116.
45. Moparthi, S.; Burrows, M.; Mgbechi-Ezeri, J.; Agindotan, B. Fusarium Spp. Associated With Root Rot of Pulse Crops and Their Cross-Pathogenicity to Cereal Crops in Montana. *Plant Dis.* **2021**, *105* (3), 548–557. https://doi.org/10.1094/PDIS-04-20-0800-RE.
46. Gaige, A. R.; Todd, T.; Stack, J. P. Interspecific Competition for Colonization of Maize Plants Between Fusarium Proliferatum and Fusarium Verticillioides. *Plant Dis.* **2020**, *104* (8), 2102–2110. https://doi.org/10.1094/PDIS-09-19-1964-RE.
47. Xi, K.; Shan, L.; Yang, Y.; Zhang, G.; Zhang, J.; Guo, W. Species Diversity and Chemotypes of Fusarium Species Associated With Maize Stalk Rot in Yunnan Province of Southwest China. *Front. Microbiol.* **2021**, *12*, 652062. https://doi.org/10.3389/fmicb.2021.652062.
48. Summerell, B. A.; Salleh, B.; Leslie, J. F. A Utilitarian Approach to Fusarium Identification. *Plant Dis.* **2003**, *87* (2), 117–128. https://doi.org/10.1094/PDIS.2003.87.2.117.

49. Warham, E. J.; Butler, L. D.; Sutton, B. C. *Seed Testing of Maize and Wheat: A Laboratory Guide*; CIMMYT, 1996.
50. Bilgi, V. N.; Bradley, C. A.; Khot, S. D.; Grafton, K. F.; Rasmussen, J. B. Response of Dry Bean Genotypes to Fusarium Root Rot, Caused by Fusarium Solani f. Sp. Phaseoli, under Field and Controlled Conditions. *Plant Dis.* **2008**, *92* (8), 1197–1200.
51. Acharya, B.; Lee, S.; Rouf Mian, M. A.; Jun, T.-H.; McHale, L. K.; Michel, A. P.; Dorrance, A. E. Identification and Mapping of Quantitative Trait Loci (QTL) Conferring Resistance to Fusarium Graminearum from Soybean PI 567301B. *Theor. Appl. Genet.* **2015**, *128*, 827–838.
52. O'Donnell, K.; Kistler, H. C.; Cigelnik, E.; Ploetz, R. C. Multiple Evolutionary Origins of the Fungus Causing Panama Disease of Banana: Concordant Evidence from Nuclear and Mitochondrial Gene Genealogies. *Proc. Natl. Acad. Sci. U. S. A.* **1998**, *95* (5), 2044–2049. https://doi.org/10.1073/pnas.95.5.2044.
53. Liu, Y. J.; Whelen, S.; Hall, B. D. Phylogenetic Relationships among Ascomycetes: Evidence from an RNA Polymerse II Subunit. *Mol. Biol. Evol.* **1999**, *16* (12), 1799–1808. https://doi.org/10.1093/oxfordjournals.molbev.a026092.
54. Carbone, I.; Kohn, L. M. A Method for Designing Primer Sets for Speciation Studies in Filamentous Ascomycetes. *Mycologia* **1999**, *91* (3), 553–556.
55. Glass, N. L.; Donaldson, G. C. Development of Primer Sets Designed for Use with the PCR to Amplify Conserved Genes from Filamentous Ascomycetes. *Appl. Environ. Microbiol.* **1995**, *61* (4), 1323–1330.
56. O'Donnell, K.; Cigelnik, E. Two Divergent Intragenomic rDNA ITS2 Types within a Monophyletic Lineage of the Fungus Fusarium Are Nonorthologous. *Mol. Phylogenet. Evol.* **1997**, *7* (1), 103–116. https://doi.org/10.1006/mpev.1996.0376.
57. Guarnaccia, V.; Aiello, D.; Polizzi, G.; Crous, P. W.; Sandoval-Denis, M. Soilborne Diseases Caused by Fusarium and Neocosmospora Spp. on Ornamental Plants in Italy. *Phytopathol. Mediterr.* **2019**, *58* (1), 127–137. https://doi.org/10.14601/Phytopathol_Mediterr-23587.
58. Weir, B. S.; Johnston, P. R.; Damm, U. The Colletotrichum Gloeosporioides Species Complex. *Stud. Mycol.* **2012**, *73*, 115–180. https://doi.org/10.3114/sim0011.
59. O'Donnell, K.; Rooney, A. P.; Proctor, R. H.; Brown, D. W.; McCormick, S. P.; Ward, T. J.; Frandsen, R. J. N.; Lysøe, E.; Rehner, S. A.; Aoki, T.; Robert, V. A. R. G.; Crous, P. W.; Groenewald, J. Z.; Kang, S.; Geiser, D. M. Phylogenetic Analyses of RPB1 and RPB2 Support a Middle Cretaceous Origin for a Clade Comprising All Agriculturally and Medically Important Fusaria. *Fungal Genet. Biol. FG B* **2013**, *52*, 20–31. https://doi.org/10.1016/j.fgb.2012.12.004.
60. Zhang, Y.; Chen, C.; Mai, Z.; Lin, J.; Nie, L.; Maharachchikumbura, S. S. N.; You, C.; Xiang, M.; Hyde, K. D.; Manawasinghe, I. S. Co-Infection of Fusarium Aglaonematis Sp. Nov. and Fusarium Elaeidis Causing Stem Rot in Aglaonema Modestum in China. *Front. Microbiol.* **2022**, *13*, 930790. https://doi.org/10.3389/fmicb.2022.930790.
61. Moreira Costa, M.; Melo, M.; Carmo, F.; Moreira, G.; Guimarães, E.; Rocha, F.; Costa, S.; Abreu, L.; Pfenning, L. Fusarium Species from Tropical Grasses in Brazil and Description of Two New Taxa. *Mycol. Prog.* **2021**, *20*, 61–72. https://doi.org/10.1007/s11557-020-01658-5.
62. Lombard, L.; van Doorn, R.; Groenewald, J. Z.; Tessema, T.; Kuramae, E. E.; Etolo, D. W.; Raaijmakers, J. M.; Crous, P. W. Fusarium Diversity Associated with the Sorghum-Striga Interaction in Ethiopia. *Fungal Syst. Evol.* **2022**, *10*, 177–215. https://doi.org/10.3114/fuse.2022.10.08.
63. Vermeulen, M.; Rothmann, L. A.; Swart, W. J.; Gryzenhout, M. Fusarium Casha Sp. Nov. and F. Curculicola Sp. Nov. in the Fusarium Fujikuroi Species Complex Isolated from Amaranthuscruentus and Three Weevil Species in South Africa. *Diversity* **2021**, *13* (10), 472. https://doi.org/10.3390/d13100472.
64. Laraba, I.; Kim, H.-S.; Proctor, R. H.; Busman, M.; O'Donnell, K.; Felker, F. C.; Aime, M. C.; Koch, R. A.; Wurdack, K. J. Fusarium Xyrophilum, Sp. Nov., a Member of the Fusarium Fujikuroi Species Complex Recovered from Pseudoflowers on Yellow-Eyed Grass (Xyris Spp.) from Guyana. *Mycologia* **2020**, *112* (1), 39–51. https://doi.org/10.1080/00275514.2019.1668991.
65. Proctor, R. H.; Van Hove, F.; Susca, A.; Stea, G.; Busman, M.; van der Lee, T.; Waalwijk, C.; Moretti, A.; Ward, T. J. Birth, Death and Horizontal Transfer of the Fumonisin Biosynthetic Gene Cluster during the Evolutionary Diversification of Fusarium. *Mol. Microbiol.* **2013**, *90* (2), 290–306. https://doi.org/10.1111/mmi.12362.
66. Sandoval-Denis, M.; Guarnaccia, V.; Polizzi, G.; Crous, P. W. Symptomatic Citrus Trees Reveal a New Pathogenic Lineage in Fusarium and Two New Neocosmospora Species. *Persoonia* **2018**, *40*, 1–25. https://doi.org/10.3767/persoonia.2018.40.01.

67. Katoh, K.; Standley, D. Katoh K, Standley DM.. MAFFT Multiple Sequence Alignment Software Version 7: Improvements in Performance and Usability. Mol Biol Evol 30: 772-780. *Mol. Biol. Evol.* **2013**, *30*. https://doi.org/10.1093/molbev/mst010.
68. Kumar, S.; Stecher, G.; Tamura, K. MEGA7: Molecular Evolutionary Genetics Analysis Version 7.0 for Bigger Datasets. *Mol. Biol. Evol.* **2016**, *33* (7), 1870–1874. https://doi.org/10.1093/molbev/msw054.
69. Swofford, D.; Sullivan, J. Phylogeny Inference Based on Parsimony and Other Methods with PAUP. *Phylogenetic Handb. Pract. Approach Phylogenetic Anal. Hypothesis Test.* **2009**, 267–312.
70. Ronquist, F.; Teslenko, M.; Mark, P.; Ayres, D.; Darling, A.; Höhna, S.; Larget, B.; Liu, L.; Suchard, M.; Huelsenbeck, J. MrBayes 3.2: Efficient Bayesian Phylogenetic Inference and Model Choice Across a Large Model Space. *Syst. Biol.* **2012**, *61*, 539–542. https://doi.org/10.1093/sysbio/sys029.
71. Nylander, J. A. A.; Ronquist, F.; Huelsenbeck, J. P.; Nieves-Aldrey, J. L. Bayesian Phylogenetic Analysis of Combined Data. *Syst. Biol.* **2004**, *53* (1), 47–67. https://doi.org/10.1080/10635150490264699.
72. Fisher, N. L.; Burgess, L. W.; Toussoun, T. A.; Nelson, P. E. Carnation Leaves as a Substrate and for Preserving Cultures of Fusarium Species. *Phytopathology* **1982**, *72* (1), 151–153.